The Plant Cell, Vol. 23: 4025–4040, November 2011, www.plantcell.org

AXY8 Encodes an α-Fucosidase, Underscoring the Importance of Apoplastic Metabolism on the Fine Structure of *Arabidopsis* Cell Wall Polysaccharides [W] [OA]

Markus Günl,[a,1] Lutz Neumetzler,[b,1] Florian Kraemer,[a] Amancio de Souza,[a] Alex Schultink,[a] Maria Pena,[c] William S. York,[c] and Markus Pauly[a,2]

[a] University of California, Berkeley, California, 94720
[b] Max-Planck-Institute for Molecular Plant Physiology, D-14476 Potsdam-Golm, Germany
[c] Complex Carbohydrate Research Center, University of Georgia, Athens, Georgia 30602

An *Arabidopsis thaliana* mutant with an altered structure of its hemicellulose xyloglucan (XyG; *axy-8*) identified by a forward genetic screen facilitating oligosaccharide mass profiling was characterized. *axy8* exhibits increased XyG fucosylation and the occurrence of XyG fragments not present in the wild-type plant. *AXY8* was identified to encode an α-fucosidase acting on XyG that was previously designated FUC95A. Green fluorescent protein fusion localization studies and analysis of nascent XyG in microsomal preparations demonstrated that this glycosylhydrolase acts mainly on XyG in the apoplast. Detailed structural analysis of XyG in *axy8* gave unique insights into the role of the fucosidase in XyG metabolism in vivo. The genetic evidence indicates that the activity of glycosylhydrolases in the apoplast plays a major role in generating the heterogeneity of XyG side chains in the wall. Furthermore, without the dominant apoplastic glycosylhydrolases, the XyG structure in the wall is mainly composed of XXXG and XXFG subunits.

INTRODUCTION

The cells of plants are encased in a wall consisting of various polymer networks. One of the dominant components in the primary plant cell wall (i.e., the wall of growing cells) in dicots and nonpoacean monocots is the hemicellulosic polysaccharide xyloglucan (up to 30% dry weight) (Hayashi, 1989; Scheller and Ulvskov, 2010). Xyloglucan (XyG) is also present but to a lesser extent in the walls of grasses (Gibeaut et al., 2005). XyG associates noncovalently with cellulose microfibrils (Bauer et al., 1973), forming a cellulose-XyG network that has been hypothesized to be the load-bearing structure of the cell (Fry, 1989). The metabolism of XyG in the wall is thought to play a significant role in turgor-driven cell expansion (Cosgrove, 2005). The main enzymes involved in apoplastic XyG metabolism are endoglucanases cleaving XyG and generating XyG oligosaccharides that may act as signals (Takeda et al., 2002) and expansins, proteins that are known to cause cell wall creep (Cosgrove, 2005). In addition, XyG endotransglycosylases (XETs) cut and religate XyG polymers either to remodel XyG in the wall or to incorporate newly synthesized XyG (Smith and Fry, 1991; Nishitani and Tominaga, 1992; Vissenberg et al., 2005). It is thus thought that the finely orchestrated action of these enzymes is associated with cell elongation (Pauly et al., 2001). The view that XyG has an important function as a plant growth regulator has recently been challenged as an *Arabidopsis thaliana* mutant whose walls are devoid of any detectable XyG is not affected in overall plant growth, development, and/or morphology, with the exception of deformed root hairs (Cavalier et al., 2008). However, it should be noted that the cellulose microfibrils in this mutant are unevenly spaced (Anderson et al., 2010); hence, it is likely that there are further hitherto unknown structural changes present in those mutant walls that functionally compensate for the loss of this dominant polysaccharide. Hence, the precise function of XyG in the plant cell wall is still under debate.

The structure of XyG has been relatively well described. On a macromolecular level, XyG embedded in the wall occurs in connected domains (Pauly et al., 1999a). One domain of the polymer acts as an enzyme-accessible microfibril tether, while another domain of the polymer is tightly associated with the cellulose microfibril via H-bonds and thus has only limited or no accessibility to enzymes. A third domain is located within the microfibril, making it inert to further modification. On a fine structural level, XyG consists of a β-1,4-linked glucan chain that is decorated with various heterogeneous side chains depending on plant species and tissue type (York et al., 1996; Obel et al., 2009). The pattern of XyG substitutions of each backbone glucosyl residue is described using a single-letter nomenclature (Fry et al., 1993). The letter G describes an unsubstituted backbone β-D-Glc*p* residue, whereas X denotes a backbone Glc unit substituted with a xylosyl-residue [i.e., an α-D-Xyl*p*-(1-6)-β-D-Glc*p* moiety]. In many dicots, such as *Arabidopsis*, the xylosyl residue can be further substituted with a β-D-Gal*p* residue (L side chain), which is often

[1] These authors contributed equally to this work.
[2] Address correspondence to mpauly69@berkeley.edu.
The author responsible for distribution of materials integral to the findings presented in this article in accordance with the policy described in the Instructions for Authors (www.plantcell.org) is: Markus Pauly (mpauly69@berkeley.edu).
[W] Online version contains Web-only data.
[OA] Open Access articles can be viewed online without a subscription.
www.plantcell.org/cgi/doi/10.1105/tpc.111.089193

further decorated with an α-L-Fuc*p* residue (F side chain) and/or an *O*-acetyl-substituent (Kiefer et al., 1989; Pauly et al., 2001). The presence of the *O*-acetyl-substituent is shown by underlining the respective one-letter code (Hoffman et al., 2005). Major insight into XyG structure has been obtained by enzymatic digestion of the XyG polymer with an endoglucanase (Guillén et al., 1995). These studies have revealed that XyG is composed of various structurally diverse oligosaccharides (Lerouxel et al., 2002). The substitution pattern of XyG has implications for the solution properties of the polymer and interactions with cellulose (Levy et al., 1997). However, the origin of the side chain diversity or the order of the oligosaccharides within the XyG polymer is not known, presenting a major impediment to understanding the XyG structure and metabolism in planta.

Much of our knowledge of XyG metabolism and function in planta has been gained through the identification and characterization of plant mutants. In addition, these mutants yielded essential information about the molecular machinery of XyG biosynthesis, which occurs in the Golgi apparatus (Moore et al., 1991; Scheible and Pauly, 2004). A forward genetic screen based on wall monosaccharide composition led to the identification of several *Arabidopsis mur* mutants altered in their XyG structure (Reiter et al., 1997). *MUR1-MUR3* encode polypeptides involved in XyG biosynthesis: *MUR1* is a GDP-mannose-2,4-dehydratase responsible for the synthesis of the precursor GDP-L-fucose (Bonin et al., 1997), *MUR2* is a XyG:fucosyltransferase (Vanzin et al., 2002), and *MUR3* is a XyG:galactosyltransferase (Madson et al., 2003). All of the *mur* mutants displayed XyG structures with altered side chain substitutions. Other XyG biosynthesis mutants have been identified through reverse genetic approaches, including various XyG:xylosyltransferase mutants (Cavalier et al., 2008; Zabotina et al., 2008). Another forward genetic screen aimed to identify mutants with defined altered XyG structures (*axy* mutants; Neumetzler, 2010; http://paulylab.berkeley.edu/axy-mutants.html). The screen was performed on a chemically mutagenized *Arabidopsis* population and was based on oligosaccharide mass profiling (OLIMP) of XyG (Lerouxel et al., 2002). OLIMP entails the profiling of XyG by treatment of *Arabidopsis* walls with a XyG-specific hydrolase (XEG; Pauly et al., 1999b) and subsequent analysis of the resulting XyG oligosaccharides via mass spectrometry (MS).

While the *axy4* mutant is described elsewhere (Gille et al., 2011), here we characterize *axy8* and related mutants, which exhibit XyG oligosaccharide profiles containing an increased abundance of fucosylated XyG side chains as well as unusual oligosaccharides that are not found in wild-type plants.

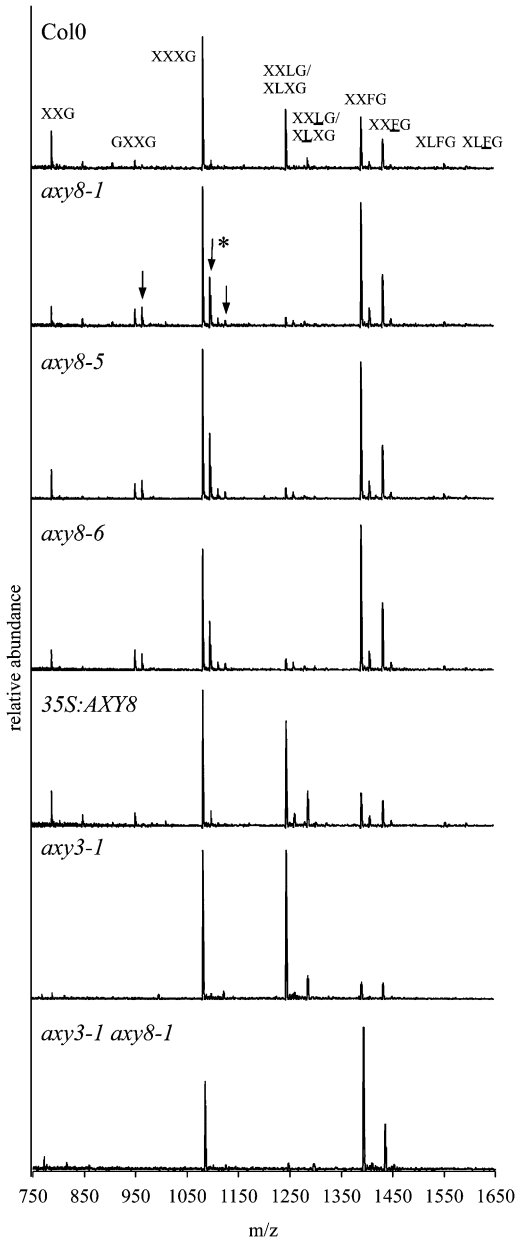

Figure 1. OLIMP Analysis.

OLIMP spectra of etiolated seedlings of the wild type (Col-0), *axy8* mutants, *AXY8* overexpression (*35S:AXY8*), the *xyl1* mutant (*axy3-1*), and a *xyl1 axy8* double mutant (*axy3-1 axy8-1*). Arrows indicate unusual XyG oligosaccharides in *axy8*. Isotopic resolution is shown in Supplemental Figure 1 online for the ions marked with an asterisk. Quantitative statistical analysis of OLIMP data is presented in Supplemental Table 1 online.

RESULTS

AXY8 Encodes a Ubiquitously Expressed Apoplastic XyG: α-Fucosidase

Screening of an ethyl methanesulfonate (EMS)–mutagenized plant population by oligosaccharide mass profiling (OLIMP; Lerouxel et al., 2002) identified a mutant, termed *axy8-1*, that exhibit significant changes in its XyG structure (Figure 1; see Supplemental Table 1 online). *axy8-1* showed increased abundance of fucosylated XyG oligosaccharides, but more importantly, OLIMP indicated ions representing oligosaccharides that have not been observed in wild-type OLIMP spectra (Figure 1, arrows; see Supplemental Figure 1 online).

The gene responsible for the observed XyG oligosaccharide phenotype in *axy8* mutants was isolated using a combination of strategies. Initially, an *axy8-1* mapping population was established by crossing *axy8-1* (Columbia-0 [Col-0] background) to the

Arabidopsis Landsberg *erecta* ecotype. After self-pollination, the resulting F2 hypocotyls were subjected to XyG OLIMP. Out of 60 hypocotyls, 48 displayed wild-type Col-0 XyG profiles, while 12 showed the characteristic *axy8* XyG profile. A χ^2 value of 0.8 is consistent with a 3:1 segregation ratio model indicative of a nuclear-encoded, monogenic, recessive trait. To narrow down the genomic region of the responsible mutation, a bulk segregant analysis by a microarray-based mapping approach was performed (Hazen et al., 2005). The analysis of the hybridization data pinpointed the mutation to the distal end of chromosome IV, between 15.5 and 17 Mbp (see Supplemental Figure 2A online). Further fine-mapping performed by PCR-based mapping of individual recombinants delimited the mutation between marker F10M10 at position 16.37 Mb and nga1139 at 16.44 Mb (see Supplemental Figure 2B online). This genomic region encompasses 24 genes, all of which were sequenced in *axy8-1*. A point mutation G→A was identified in the locus At4g34260, resulting in a premature stop codon in the third exon of the gene (TGG^{1254} to TGA^{1254}, Trp418Stop; Figure 2A).

In the OLIMP screen, several mutants with the *axy8* phenotype were found (Neumetzler, 2010), and At4g34260 was sequenced in all those mutants (Figure 2A). All *axy8* mutants exhibit mutations in this gene locus, including mis-sense mutations (*axy8-3*, Pro562-Leu; *axy8-4*, Cys511Tyr) and additional non-sense mutations (*axy8-2*, Arg398Stop; *axy8-7*, Trp441Stop; Figure 2A). To confirm further that At4g34260 coincides with the *AXY8* locus, T-DNA insertion lines were obtained (*axy8-5* and *axy8-6*) and their XyG OLIMP phenotype determined (Figure 1; see Supplemental Table 1 online). Whereas the *AXY8* transcript is still present in those lines, albeit in reduced abundance (Figure 2B), both displayed the characteristic *axy8* XyG oligosaccharide profile of a higher abundance of fucosylated oligosaccharides and the presence of the unusual oligosaccharides (Figure 1; see Supplemental Table 1 online). In addition, the genomic sequence of wild-type *AXY8* was placed under the control of the constitutive 35S promoter and transformed into Col-0. Indeed, the XyG oligosaccharide profile was restored to the wild type in terms of absence of unusual oligosaccharides and a reduction XyG fucosylation level (Figure 1; see Supplemental Table 1 online). In summary, these data provide conclusive evidence that *AXY8* is represented by At4g34260.

AXY8 encodes a protein consisting of 843 amino acids with a calculated molecular mass of 93.7 kD (The Arabidopsis Information Resource; www.Arabidopsis.org), including a potential 27–amino acid signal peptide (probability 0.905; http://www.cbs.dtu.dk/services/SignalP/). The protein is not predicted to contain any transmembrane domains (http://aramemnon.uni-koeln.de/; Schwacke et al., 2003) or a glycosylphosphatidylinositol anchor (http://gpi.unibe.ch/; Fankhauser and Mäser, 2005). AXY8 has been designated Fuc95A, as it belongs to a glycosylhydrolase family 95 (www.cazy.org). When expressed heterologously in tobacco (*Nicotiana tabacum*), it exhibits α-fucosidase activity not only against a model compound, 2-fucosyl-lactose, but also against XyG oligosaccharides as it converts XXFG to XXLG and releases fucosyl residues from the XyG polymer (Léonard et al., 2008). This designation is consistent with the observed increase in fucosylated XyG oligosaccharides in the *axy8* mutants due to a nonfunctional fucosidase. Hence, the impact of AXY8 on overall fucosidase activity present in *Arabidopsis* was assessed. Protein

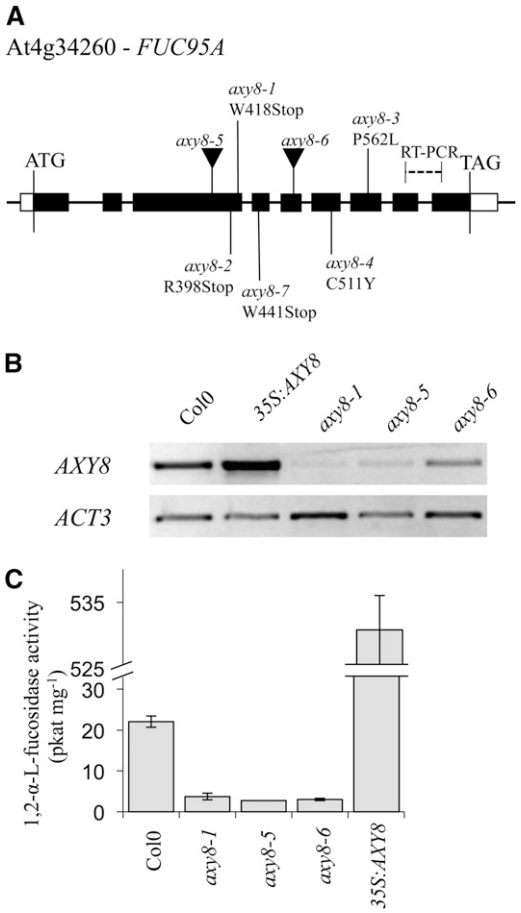

Figure 2. axy8 Mutants: Genetic Properties and Activity.

(A) Gene model of At4g34260, including the location of the non-sense and mis-sense mutations and T-DNA insertions of the various *axy8* alleles. The location of the amplicon for RT-PCR of *AXY8* (see **[B]**) is shown as a dotted line; black rectangles indicate exons, white rectangles indicate the untranslated regions, and black lines indicate introns.

(B) RT-PCR transcript analysis of *AXY8* in etiolated seedlings of the various *axy8* mutants, *AXY8* overexpression line (*35S:AXY8*), and Col-0 wild type using *ACTIN3* (*ACT3*) as an internal control.

(C) The 1,2-α-L-fucosidase activity in extracts of etiolated seedlings obtained from various *axy8* mutants, the *AXY8* overexpression line (*35S*:*AXY8*), and Col-0 wild type. The 1,2-α-L-fucosidase activity was tested against 2-fucosyllactose (n = 3, ±SD). pkat, picokatal.

extracts from various *axy8* mutants (EMS and T-DNA insertion lines) were tested for fucosidase activity against 2-fucosyl-lactose; indeed, a >80% drop in activity was observed in all mutants (Figure 2C). The data provide further evidence that *AXY8* encodes a fucosidase represented by At4g34260.

By contrast, constitutive expression of AXY8 led to a 24-fold increase in fucosidase activity in plant extracts. The dominance of AXY8 as a source of plant fucosidase activity is consistent with its ubiquitous expression, as shown by *AXY8* promoter–β-glucuronidase (GUS) fusion analysis (see Supplemental Figure 3 online). In etiolated seedlings, where the *axy8* XyG oligosaccharide phenotype was observed, *AXY8* seems to be expressed

in all tissues, including all cell layers of the hypocotyl. In adult plants, expression seems to be strongest in vascular tissue, in leaf trichomes, in the root elongation zone, and in emerging lateral roots, but it is also present in other tissues at a low level (see Supplemental Figure 3 online). Consistent with the ubiquitous expression of AXY8 is the data obtained from XyG OLIMP analysis of various plant tissues (see Supplemental Figure 4 online) demonstrating the presence of the *axy8* structural XyG phenotype, higher fucosylation levels, and unusual XyG oligosaccharides in leaves and flowers.

The subcellular localization of the fucosidase AXY8 was investigated by transient expression of its green fluorescent protein (GFP) fusion constructs in tobacco epidermal cells (Figure 3; see Supplemental Figure 5 online). The AXY8-GFP fusion was present in the apoplast and was retained in the apoplast when the plasma membrane, as indicated by the marker FM 4-64, receded under plasmolysis-inducing conditions (Figure 3J; see Supplemental Figure 5 online). These experiments confirmed earlier reports that AXY8 represents a soluble protein (Léonard et al., 2008) and that plant fucosidase activities can be found in apoplastic extracts of plants (de la Torre et al., 2002; Franková and Fry, 2011).

Apoplastic proteins are translated into the lumen of the endoplasmic reticulum, transiently move through the Golgi apparatus, and are exported via exocytosis into the apoplast. Hence, there is a possibility that the fucosidase protein might come in contact with XyG in the Golgi apparatus. To assess if the fucosidase acts on XyG in the Golgi, a microsomal preparation was generated from etiolated seedlings, essentially separating microsomes from the cell wall (Obel et al., 2009). The XyG structure in both fractions was assessed by OLIMP (Figure 4). Both fractions harbor similar XyG oligosaccharide structures in *axy8*. However, in the wild-type (Col-0) wall preparation, fucosylated XyG oligosaccharides (allF; see Supplemental Table 1 online) are reduced in relative abundance compared with the microsomal preparations. This is consistent with the action of a fucosidase in the apoplast. *axy8* microsomes contain a higher degree of fucosylated XyG oligosaccharides than do Col-0 microsomes, suggesting that the fucosidase can act to some extent already in the microsomes. However, it appears that AXY8 is mainly active in the apoplast, as wall XyG from *axy8* contains 60% more fucosylated XyG oligosaccharides compared with Col-0 (see Supplemental Table 1 online). Furthermore, the abundance of fucosylated XyG oligosaccharides in the *axy8* mutant remains constant in the wall fraction compared with the microsome fraction, again consistent with a lack of apoplastic fucosidase action (Figure 4; see Supplemental Table 1 online).

In summary, the data are consistent with AXY8 representing an α-fucosidase that acts on XyG once deposited in the cell wall. Furthermore, the unusual oligosaccharides present in *axy8* (Figure 4, arrows) occur only in the wall fraction, not the microsomal fraction, indicating that they arise through metabolism of XyG in the apoplast rather than biosynthesis in the Golgi apparatus.

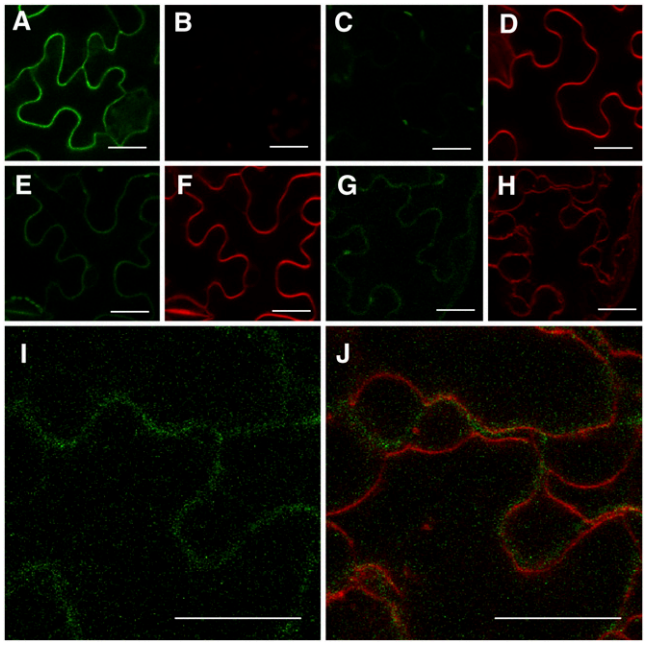

Figure 3. Transient Expression of p35S:AXY8-GFP in *Nicotiana benthamiana*.

Infiltration of p35S:AXY8-GFP showing GFP channel **(A)** and FM 4-64 (plasma membrane marker) channel **(B)**. Infiltration of FM 4-64 showing GFP channel **(C)** and FM 4-64 channel **(D)**. Coinfiltration of p35S:AXY8-GFP and FM 4-64 showing GFP channel **(E)** and FM 4-64 channel **(F)**. Coinfiltration of p35S:AXY8-GFP and FM 4-64 under plasmolysis-inducing conditions with 1 M mannitol showing GFP channel (**[G]**; enlarged in **[I]**), FM 4-64 channel **(H)**, and enlarged merge of both channels **(J)**. Images were acquired with a Zeiss LSM 710. Bars = 25 μm.

Axy8 Contains Underxylosylated XyG Fragments

The XyG structure in *axy8* is distinctly different from wild-type XyG in three aspects (Figure 5B). An increase in the fucosylated XyG oligosaccharide XXFG is observed along with a concomitant decrease in the abundance of XXLG and unusual small XEG-generated ions (mass-to-charge ratio [*m/z*] <1700) that are not present in wild-type XEG extracts, with *m/z* 967, 1099, and 1129. In addition, when extending the mass range of the mass spectrometer, other XEG-generated ions appear that are much larger than the usual XyG oligosaccharides found in plants with *m/z* of 1849, 2011, 2025, 2158, and 2319.

To determine the structure of the unusual small XyG oligosaccharides, an attempt was made to purify or at least enrich them for subsequent analysis. Using a combination of size-exclusion chromatography followed by reversed phase chromatography, fractions could be collected whose major components were these unusual XyG oligosaccharides: in the case of fraction 1, *m/z* 967 and 1129; in the case of fraction 2, *m/z* 1099 coeluting with the regular XyG oligosaccharides *m/z* 1085 (XXXG) and 1247 (XLXG/XXLG; Figure 6A). The mass of all four unusual ions is consistent with a sugar composition of a single deoxyhexose, one or two pentoses, presumably Xyl, and various contents of hexoses (805, $Hexose_3Pentose_1Deoxy_1$; 967, $Hexose_4Pentose_1Deoxy_1$;1099, $Hexose_4Pentose_2Deoxy_1$; 1129, $Hexose_5Pentose_1Deoxy_1$). Since MS cannot determine the nature of the deoxyhexosyl or hexosyl residues, ^{1}H-NMR was used on the two fractions to gain further insight into the structures of these unusual

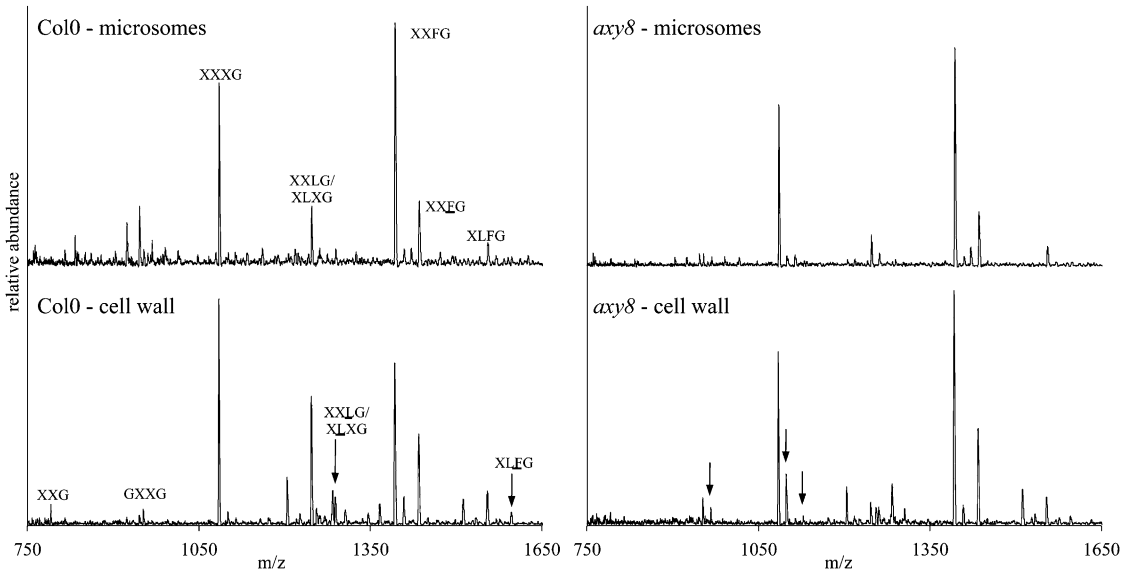

Figure 4. Comparison of XyG Oligosaccharide Profiles Generated by OLIMP from Cell Walls and a Microsome Preparation of the Same Etiolated Hypocotyl Material.

Quantitative statistical analysis of OLIMP data is presented in Supplemental Table 1 online. Arrows indicate unusual XyG oligosaccharides found in *axy8* (Figure 1).

oligosaccharides (Perrin et al., 2003; Hoffman et al., 2005; Figure 6B). The ^{1}H-NMR spectrum of the wild-type XyG oligosaccharides contained resonances at δ 5.273 (H-1 of α-L-Fuc*p*), δ 5.145 (H-1 of 2-linked α-D-Xyl*p*), and δ 5.616 (H-1 of 2-linked β-D-Gal*p*), diagnostic for the presence of the α-L-Fuc*p*-(1→2)-β-D-Gal*p*-(1→2)-α-D-Xyl*p* side chain at O6 of a β-D-Glc*p* residue at any position in the oligosaccharide except the nonreducing end. The spectrum of the *axy8* XyG oligosaccharides contained these resonances along with additional resonances (δ 5.287, δ 5.137, and δ 4.621) diagnostic for the presence of structures such as FG and FGG, which have fucosylated side chains at O6 of the β-D-Glc*p* residue at the nonreducing end (Spronk et al., 1997). Based on this information, the most probable structure for $Hexose_3$-$Pentose_1Deoxy_1$ is FG. Furthermore, the spectrum of the *axy8* XyG oligosaccharides contains a resonance at δ 4.476, characteristic of a nonreducing terminal Glc linked to a Glc residue bearing a fucosylated side chain, such as in GFG, which has been isolated from apple (*Malus domestica*) XyG (Spronk et al., 1997). These resonances are consistent with the structure GFG for the oligosaccharide with the composition $Hexose_4Pentose_1Deoxy_1$. However, the presence of the structure FGG cannot be ruled out without purification of the oligosaccharides. Similarly, the oligosaccharide $Hexose_5Pentose_1Deoxy_1$ may correspond to the structures GFGG, GGFG, and/or FGGG. The NMR spectrum of fraction 2 (Figure 6B) is very similar to a control XyG oligosaccharide sample obtained by XEG digest of wild-type walls. This is not surprising, as the major XyG oligosaccharides are XXXG and XLXG/XXLG. However, it also contains resonances at δ 5.273, δ 5.145, and δ 4.616 characteristic of oligosaccharides with a fucosylated side chain at O6 of the β-D-Glc*p* residue next to the reducing end. Based on the NMR data, the most probable structure for the oligosaccharide in this fraction is XFG ($Hexose_4Pentose_2Deoxy_1$). In summary, the unusual XyG oligosaccharides present in *axy8* do not appear to be novel XyG structures but rather truncated versions of fucosylated XyG oligosaccharides with backbone structures having fewer than the usual four glucosyl units. The data also indicate that the Xyl content of the *axy8* XyG is reduced compared with the wild type.

An attempt was made to elucidate the structures of the large (>1700 D) unusual XEG released XyG oligosaccharides not found in wild-type *Arabidopsis*. It was noted that while these oligosaccharides are present after an XEG digest of *axy8* walls, they were absent when digesting *axy8* wall preparations with a commercial endo-β-1,4-glucanase (EG; Figure 5C). Other features of the *axy8* XyG structure remained upon EG digestion (i.e., the smaller unusual oligosaccharides described above and a higher degree of XyG fucosylation). In particular, the unusual XyG oligomer consistent with a structure of GFG was very prevalent (Figure 5C; see Supplemental Table 1 online). Therefore, the large XyG oligosaccharides have structural properties that allow them to be hydrolyzed with EG but not XEG. Using high-performance anion exchange chromatography (HPAEC) with subsequent matrix-assisted laser desorption ionization–time of flight (MALDI-TOF) analysis, a fraction could be collected that was enriched in these larger XyG oligosaccharides (Figure 5D). Based on the mass, the likely side chain composition (G, X, or F) could be assigned. When using these putative compositions, the oligosaccharides would have a backbone of between six and seven glucosyl units. However, the order of the side chains could not be ascertained by MS. To gain more insight into the order of the side chains, the enriched large XyG oligosaccharides were reduced with deuterated $NaBD_4$ to their respective alditols (-ol; Figure 5D)

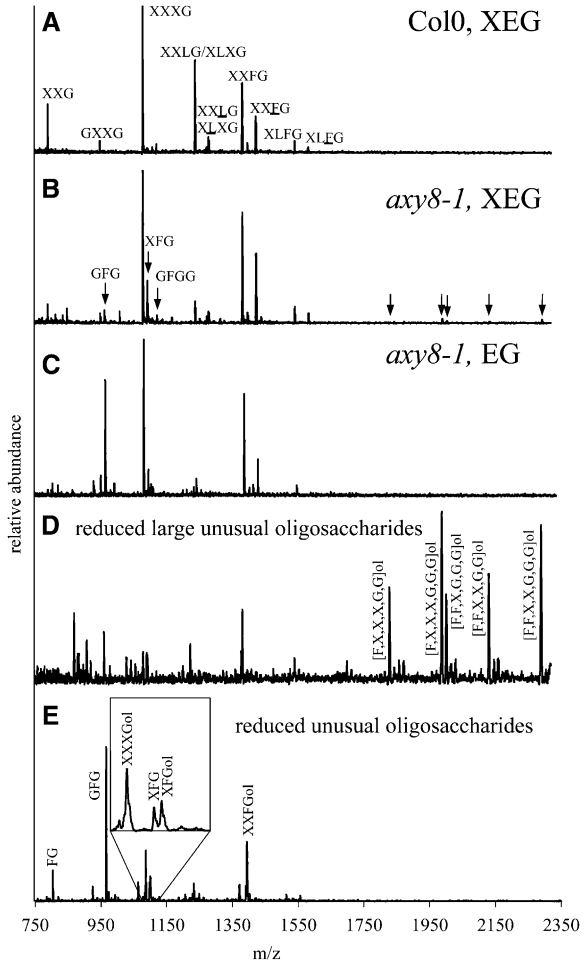

Figure 5. OLIMP Analysis of XyG Oligosaccharides Released from Walls.

One-letter code XyG oligosaccharide nomenclature according to Fry et al. (1993). Parentheses indicate potential composition of XyG oligosaccharides based on *m/z* of the ions.

(A) OLIMP of an XEG digest of wild-type (Col-0) etiolated seedlings.

(B) OLIMP of an XEG digest of *axy8-1* etiolated seedlings. Arrows indicate unusual XyG oligosaccharides that are not detected in Col-0.

(C) OLIMP of an EG digest of *axy8-1* etiolated seedlings.

(D) Mass spectrum of a XEG digest fraction enriched for XyG oligosaccharides that are larger than ~1700 D after reduction to their corresponding alditols.

(E) Mass spectrum of oligosaccharides in **(D)** further digested with EG. Proposed structures are placed on top of the ions. Statistical analysis of OLIMP data is presented in Supplemental Table 1 online.

specifically labeling the reducing end of the large oligosaccharides. They were then digested with EG (Figure 5E). The ions of the resulting reduced XyG oligosaccharides are consistent with the regular XyG oligosaccharides found in *Arabidopsis* XyG, XXXG and XXFG. The resulting nonreduced XyG is consistent with the unusual XyG oligosaccharides observed in *axy8*, FG and GFG. One oligosaccharide consistent with XFG was found in both reduced and unreduced form. Hence, the likely structures of the large XyG oligosaccharides are FG-XXXG or FG-XXFG, GFG-XXXG or GFG-XXFG, or XFG-XFG and GFG-XFG. All of those cases have in common that a fucosylated XyG fragment resides on the nonreducing end and an oligosaccharide with an X residue on the reducing end. However, whereas these are the most likely side chain scenarios, other side chain distributions cannot be excluded. In any case, it is clear that the large unusual XyG fragments contain the smaller unusual XyG fragments not present in *Arabidopsis* wild-type walls.

The absolute amount of XyG present in the walls can be determined by HPAEC-pulsed amperometric detection (PAD) using an XXXG standard curve (see Supplemental Figure 6 online; Table 1). Since XEG does not release all XyG present in the walls (Pauly et al., 1999a), an extraction with alkali was performed to capture the structure of as much XyG as possible (Table 1). Based on these data, the total amount of the unusual XyG fragments (small and part of the large oligosaccharides) make up ~19% of all XyG oligosaccharides released by enzyme (XEG; Table 1). Total XyG stripped of microfibrils using alkali contain only 7% of these XyG fragments, while XyG in the alkali fraction after enzymatic predigestion contains only 4% of these fragments. Hence, the fragments are dominant in an enzyme-accessible domain of XyG in the wall, hinting that they might be derived through apoplastic enzymes. Whereas the total amount of XyG present in the wall is not significantly different between wild-type and *axy8* walls (Table 1; 4 M KOH extractable XyG), there is a significantly larger proportion of XyG that can be extracted with the enzyme XEG from *axy8* walls (Table 1; XEG-accessible XyG) and a concomitant lower amount of XyG remaining in the wall after the enzyme pretreatment (Table 1; 4 M KOH-extractable XyG after XEG digestion). Therefore, inactivating a fucosidase as in *axy8* leads to an increase in enzyme-accessible XyG.

The dominant structural feature of *axy8* XyG is its increase in fucosylation. Given the lack of a fucosidase activity in *axy8*, this is not surprising. The total amount of fucosylated XyG oligosaccharides including the unusual fucosylated XyG fragments is increased from 39% in wild-type *Arabidopsis* XyG to 54% in *axy8* XyG (Table 1; 4 M KOH extractable XyG). This increase is independent of the XyG domain, as the enzyme-accessible domain (31% wild type to 63% in *axy8*; XEG; Table 1) and the remaining alkali-extractable domain (42 to 54%; 4 M KOH after XEG) display an increase in fucosylation. The quantitative analysis of XyG oligosaccharides by HPAEC allows also the separation of the structural isomers XLXG and XXLG unlike MS methods such as OLIMP (see Supplemental Figure 6A online). The oligosaccharide XXLG is drastically reduced in *axy8-1* compared with wild-type seedling walls (Table 1), by 64% (5.0 to 1.8 μg mg^{-1}) in total alkali extractable XyG; again, in both XyG domains, 78% in the XEG accessible domain and 66% in the XyG domain closely attached to the cellulose microfibrils.

A XyG:α-Xylosidase Is Required for the Generation of the Unusual XyG Fragments in *axy8*

The origin of the unusual XyG oligosaccharides was assessed using a genetic approach. One hypothesis is that these fragments are the result of partial degradation of XyG. For this to occur, other glycosidases would be necessary. One prominent

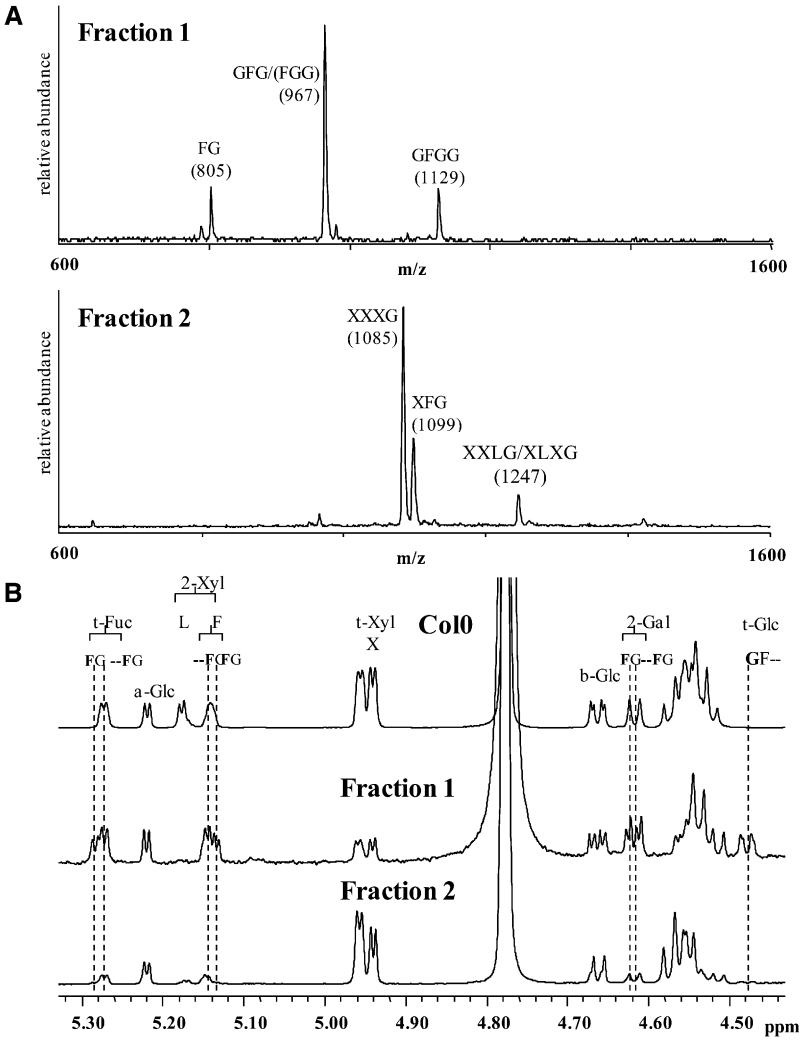

Figure 6. Structure of Unusual XyG Oligosaccharides.

(A) MALDI-TOF mass spectra of fractions 1 and 2 of partially purified XyG oligosaccharides isolated from *axy8* (for purification details, see Methods). *m/z* of the most abundant ions and their proposed structures (see **[B]**) are highlighted.

(B) Anomeric regions of the ^{1}H-NMR spectra of XyG oligosaccharides obtained by XEG digest from wild-type plants and fractions 1 and 2 of partially purified XyG oligosaccharides from *axy8*. The residues corresponding to each group of anomeric proton resonances are indicated at the top of the graphs. The location of each of these residues in particular side chains (X, L, or F), along with the location of the side chain in the oligomer, is indicated below the brackets. FG, fucosylated side chains at O6 of the β-D-Glc*p* residue at the nonreducing end; –FG, fucosylated side chain at O6 of a β-D-Glc*p* residue at any position except the nonreducing end; GF, nonreducing terminal Glc linked to a Glc residue bearing the fucosylated side chain.

glycosidase would be an α-xylosidase, as this enzyme is the first enzyme to remove the xylosyl residue from the nonreducing end of a XyG polymer or oligomer (Guillén et al., 1995; Iglesias et al., 2006). Therefore, *axy8-1*, the fucosidase mutant, was crossed with *axy3-1*, a mutant with an inactive XyG:α-xylosidase (Günl and Pauly, 2011). XyG analysis by OLIMP and HPAEC of the double mutant indicated a complete lack of the unusual XyG fragments (small and large; Figure 1, Table 1; see Supplemental Figure 6 online). Hence, the xylosidase is required for generating these fragments. The *axy8* XyG phenotype with a higher degree of fucosylation still prevails in the double mutant. XyG in the xylosidase mutant *axy3* can be extracted to a larger extent both with enzyme and alkali (Günl and Pauly, 2011; Table 1, total XyG oligosaccharides). While still present in the double mutant in total alkali-extracted XyG and each XyG domain, it does not reach the high amounts as in *axy3* alone.

axy8 Does Not Exhibit Changes in Other Wall Monosaccharides nor in Plant Growth or Morphology

The overall cell wall structure of the *axy8* mutants was assessed beyond XyG. The monosaccharide composition of the matrix polysaccharides showed an increase in wall Fuc levels in all *axy8* alleles tested and a corresponding decrease in wall Fuc levels in

Table 1. Quantification of XyG Oligosaccharides of Etiolated Seedlings by HPAEC-PAD

XyGO Composition ($\mu g\ mg^{-1}$)										
Arabidopsis Plant	Total Alkali-Extractable XyG									
	XXG	XXXG	XXLG	XXFG	XLFG	XFG	GFGXXXG	GFGXXFG	Total F[a]	Total XyGOs
Col-0	2.0 ± 0.5	10.9 ± 0.5	5.0 ± 0.2	11.1 ± 0.7	0.5 ± 0.1	ND	ND	ND	11.6 ± 0.7	30.0 ± 1.5
axy8-1	1.3 ± 0.1	11.4 ± 0.8	1.8 ± 0.1	14.3 ± 0.9	0.7 ± 0.1	1.1 ± 0.1	0.6 ± 0.1	0.7 ± 0.0	17.3 ± 1.2	32.3 ± 2.2
axy3-1	1.6 ± 0.3	16.1 ± 1.8	12.1 ± 1.6	11.8 ± 1.4	0.7 ± 0.1	ND	ND	ND	12.5 ± 1.5	42.5 ± 5.2
axy3-1 axy8-1	1.4 ± 0.1	13.9 ± 0.7	2.6 ± 0.2	18.8 ± 0.8	0.7 ± 0.0	ND	ND	ND	19.6 ± 0.9	37.6 ± 1.8
	XEG-Accessible XyG									
	XXG	XXXG	XXLG	XXFG	XLFG	XFG	GFGXXXG	GFGXXFG	Total F[a]	Total XyGOs
Col-0	0.2 ± 0.0	1.3 ± 0.2	0.9 ± 0.1	1.0 ± 0.2	0.1 ± 0.0	ND	ND	ND	1.1 ± 0.2	3.5 ± 0.5
axy8-1	0.1 ± 0.0	1.5 ± 0.1	0.2 ± 0.0	2.0 ± 0.1	0.1 ± 0.0	0.3 ± 0.0	0.3 ± 0.0	0.3 ± 0.0	2.9 ± 0.2	4.8 ± 0.3
axy3-1	0.3 ± 0.0	4.2 ± 0.4	4.4 ± 0.4	1.3 ± 0.1	0.1 ± 0.0	ND	ND	ND	1.4 ± 0.2	10.2 ± 1.0
axy3-1 axy8-1	0.2 ± 0.0	3.4 ± 0.5	0.2 ± 0.1	4.7 ± 0.8	0.2 ± 0.0	ND	ND	ND	4.9 ± 0.8	8.7 ± 1.4
	Alkali-Extractable XyG after Removal of XEG-Accessible XyG									
	XXG	XXXG	XXLG	XXFG	XLFG	XFG	GFGXXXG	GFGXXFG	Total F[a]	Total XyGOs
Col-0	1.5 ± 0.2	10.1 ± 0.5	4.1 ± 0.3	11.0 ± 0.5	0.5 ± 0.0	ND	ND	ND	11.5 ± 0.6	27.4 ± 0.5
axy8-1	0.7 ± 0.1	9.1 ± 0.4	1.4 ± 0.1	11.8 ± 0.6	0.5 ± 0.0	0.5 ± 0.0	0.3 ± 0.0	0.3 ± 0.0	13.4 ± 0.7	24.9 ± 0.7
axy3-1	0.9 ± 0.1	12.6 ± 0.3	8.2 ± 0.3	10.4 ± 0.3	0.5 ± 0.0	ND	ND	ND	10.9 ± 0.3	32.8 ± 0.3
axy3-1 axy8-1	0.8 ± 0.2	10.3 ± 0.5	1.7 ± 0.1	14.1 ± 0.8	0.5 ± 0.0	ND	ND	ND	14.6 ± 0.8	27.4 ± 0.8

XyG oligosaccharide nomenclature according to Fry et al. (1993). The mean value of six independent XyG extractions (±SD) is shown. The amounts of XyG oligosaccharides GXXG, GFG, GFGG, FGXXXG, GFGXFG, and XFGXFG are not high enough for HPAEC-PAD quantification. ND, not detected.
[a]Total F comprises all fucosylated XyG oligosaccharides (XXFG, XLFG, XFG, GFGXXXG, GFGXXFG).

the *AXY8* overexpression line (see Supplemental Table 2 online). Other significant changes were not consistent in all *axy8* alleles. Hence, based on wall monosaccharide compositional analysis, there is no evidence of an alteration of the structure or abundance of any wall polymer other than XyG.

All *axy* mutants mentioned here with the exception of *axy3*, which has shorter siliques and lower seed set as previously described (Günl and Pauly, 2011), did not differ from *Arabidopsis* wild-type plants in terms of growth morphology of seedlings or adult plants (data not shown). The *axy3* phenotype prevailed in the *axy8-1 axy3-1* double mutant (data not shown), indicating that an apparent lack of a fucosidase does not have any impact, positive or negative, on this phenotype.

DISCUSSION

XyG is the major hemicellulose in the primary walls of dicots. Its structure is relatively well described, and it is the wall polymer about which the most information is known in terms of genes involved in its biosynthesis (Scheller and Ulvskov, 2010). Hence, we consider XyG an excellent model for studying general mechanisms of wall heteroglycan biosynthesis and metabolism.

AXY8, a Dominant Apoplastic Acting XyG:α-Fucosidase

Fucosidases acting on XyG have been studied for some time due to the proposed importance of XyG fucosylation: Fucosyl residues on XyG oligosaccharides are thought to act as signaling molecules, oligosaccharins, inhibiting auxin dependent cell elongation, whereas the nonfucosylated XyG oligosaccharides do not (York et al., 1984). Substitution of the fucosyl residue with an L-galactosyl residue has the same effect (Zablackis et al., 1996). Fucosylation of the XyG polymer is thought to impact binding to cellulose microfibrils (Levy et al., 1997). These studies established the role of XyG metabolism in cell elongation and, thus, plant growth.

Two *Arabidopsis* genes have been proposed to encode XyG: fucosidases: FXG1, as it exhibits α-fucosidase activity against XyG oligosaccharides when heterologously expressed (de la Torre et al., 2002), and Fuc95A that when expressed heterologously as previously shown is able to release Fuc from XyG oligosaccharides and polymers (Léonard et al., 2008). However, their role in planta has not been established yet. Here, we present the characterization of an *Arabidopsis* fucosidase mutant, *axy8*. AXY8 (Fuc95A; At4g34260) is the only member of the CAZY hydrolase family 95 in *Arabidopsis*. Since the fucosidase activity in the *axy8* mutant extract is reduced by >80% against the model substrate 2-fucosyl-lactose (Figure 2C) and the *axy8* phenotype has been observed in all tissues tested (Figure 1; see Supplemental Figure 4 online), AXY8 seems to be the dominant fucosidase in XyG metabolism in etiolated seedlings in vivo. What role FXG1, which is not evolutionarily related to AXY8 and has not been assigned to any CAZY glycosylhydrolase family, plays in XyG metabolism in vivo remains to be investigated.

Based on previous biochemical studies (de la Torre et al., 2002; Franková and Fry, 2011) and confirmed by GFP experiments presented here, AXY8 is localized in the apoplast (Figure 3). Based on OLIMP of microsomal fractions, it acts mainly but not exclusively on XyG after secretion into the apoplast (Figure 4; see Supplemental Table 1 online).

Trimming of XyG Side Chains by Glycosidases Is Essential to Generate Structural Diversity

XyG in *Arabidopsis* and many dicots contain only four side chain substituents (xylosyl, galactosyl, *O*-acetyl, and fucosyl residues), which are linked in a specific order: L-Fuc*p*-α-(1→2)-[acetyl-(1→6)]-D-Gal*p*-β-(1→2)-D-Xyl*p*-α-(1→6)-D-Glcp or as represented in the one-letter code, F. The glycosyltransferases, but not the acetyltransferase, that lead to these specific linkages have been identified (Scheller and Ulvskov, 2010). However, XyG is not completely composed of this unit, as for example . . . FFFF… is not found, but rather derivatives/fragments of this maximum side chain F as in X, L, F, and L. The mechanism that determines this variety of the side chain fragments is not known. Furthermore, when XyG is digested with endoglucanases, such as XEG, XyG oligosaccharides are generated with units of four side chains each, termed XXXG-type structures (Vincken et al., 1997), resulting in 11 distinct XyG oligosaccharides in *Arabidopsis* (Figure 1). Again, the mechanism that determines the order of the side chains within these oligosaccharides is not known.

In general, the fine structure of any polymer in the plant cell wall is determined by two processes: its synthesis by glycosyltransferases and its potential further modification by, for example, glycosylhydrolases. It is assumed that these two processes occur in separate cellular compartments for XyG: Synthesis occurs in the Golgi apparatus (Lerouxel et al., 2006), and modification/trimming by glycosylhydrolases occurs in the apoplast as shown here with fucosylation of XyG. Based on the XyG analysis of the double mutant *axy8 axy3* with an inactive fucosidase and xylosidase, the diversity of the XyG oligosaccharide composition can be markedly reduced to mainly two oligomers, XXXG and XXFG, in etiolated seedlings (Figure 1; see Supplemental Table 1 online). Hence, these apoplastic glycosidases play a crucial role in generating structural diversity within the XyG polymer in vivo. Lack of the fucosidase activity alone in *axy8* leads to an increase in fucosylation of XyG compared with wild-type levels (Figure 1; see Supplemental Table 1 online).The amount of XXLG in wall XyG is reduced in this mutant by nearly 80% (Table 1). XXLG is unique as it represents the substrate for the fucosyl-transferase (At-FUT1) active in the Golgi during XyG biosynthesis (Perrin et al., 1999). Apparently, in vivo this transferase activity is very potent as nearly all of the XyG is fucosylated. Heterologously expressed At-FUT1 shows strong fucosylation activity in vitro on exogenously supplied XXLG (Leboeuf et al., 2008) but not to the same level as found in vivo. Therefore, some mechanistic details of in vivo XyG fucosylation are still lacking. More importantly, it seems that glycosyltransferases involved in XyG biosynthesis in the Golgi are responsible for generating XyG with their side chain substituents but play only a minor role in creating structural side chain diversity in the wall in vivo. Whereas this statement is supported only by the data presented here on XyG fucosylation, it will be interesting to see if it applies also to other wall polymers.

The Role of AXY8 in Apoplastic XyG Metabolism

The apoplast contains numerous glycosylhydrolase activities that could lead to a complete turnover of XyG, including endoglucanases to generate XyG oligosaccharides (Hensel et al., 1991) and glycosidases (i.e., fucosidase, galactosidase, xylosidase, and glucosidase activities) (Iglesias et al., 2006). In particular a XyG:xylosidase (XYL1) has been described that removes a xylosyl residue specifically from the nonreducing end of the XyG polymer (Sampedro et al., 2001). The enzyme is expressed in elongating tissues and is auxin induced (Sánchez et al., 2003). The initial product, GXXG or GXFG, has been found in XyG in the elongation zone (Guillén et al., 1995; Pauly et al., 2001) particularly in the enzyme-accessible domain of the XyG polymer, demonstrating that XyG metabolism, including glycosylhydrolase activities, play a role in planta. A xylosidase knockout mutant, *xyl1/axy3* (Sampedro et al., 2010; Günl and Pauly, 2011), results in more accessible XyG in the wall presumably due to a lack of XyG turnover. Subsequent removal of the glucosyl residue by a glucosidase leads to the generation of XXG, a XyG oligosaccharide with a backbone of three glucosyl residues. This oligomer has also been found in plant walls (Pauly et al., 2001; Figure 1; see Supplemental Figure 4 online).

The role of a fucosidase on XyG metabolism in planta had not been investigated so far. Based on the XyG structure present in the *axy8* mutant and *axy8 axy3* double mutant, the following model of apoplastic XyG metabolism in etiolated seedlings emerges (Figure 7). XyG is secreted into the wall mainly composed of XXXG and XXFG units. In wild-type plants, XyG can in essence be completely degraded by the existing glycosidases. In the *axy8 axy3* double mutant, both xylosidase and fucosidase are inactive; hence, XyG cannot undergo any turnover. However, in the *axy8* mutant, all glycosidases are still active apart from the fucosidase, resulting in the partially degraded XyG fragments GGFG, XFG, GFG, down to FG (Figure 5). The data suggest that these unusual XyG fragments reside at the nonreducing end of the polymer, as these unusual oligosaccharides can be found at the nonreducing end of partially digested XyG dimers (Figure 5E). One exception seems to be XFG. This oligosaccharide can also be found at the reducing end of the partially digested XyG (Figure 5E). It is likely that it is incorporated into the middle of XyG through the action of apoplastic XETs. XETs are enzymes that cut and religate XyG chains or incorporate XyG oligomers into the polymer (Fry et al., 1992; Nishitani and Tominaga, 1992; Figure 7). XET has been shown to act in vivo specifically in the elongation zone (Vissenberg et al., 2000) and is thought to play a role in XyG restructuring (Thompson and Fry, 2001). Recently, it has been suggested that XETs might function in XyG biosynthesis as part of a two-phase biosynthesis mechanism; recently synthesized XyG oligosaccharides in the endomembrane system might be polymerized in the second phase in the apoplast by XETs (Fincher, 2009; Burton et al., 2010). Oligomers that are xylosylated at the nonreducing end are acceptor substrates for XETs, whereas nonxylosylated oligosaccharides, such as GXXG, GFG, or FG, are not, at least with in vitro assays (Lorences and Fry, 1993). Hence, *axy8* provides in vivo evidence that degradation of the XyG backbone via xylo- and glucosidases occurs only or dominantly from the nonreducing end of a polymer.

Other features of the XyG structure that are based on a lack of glycosidase activity are that the XyG abundance remains constant in the wall, but a larger proportion is in the enzyme-accessible domain of XyG (Table 1). This increase of enzyme-accessible

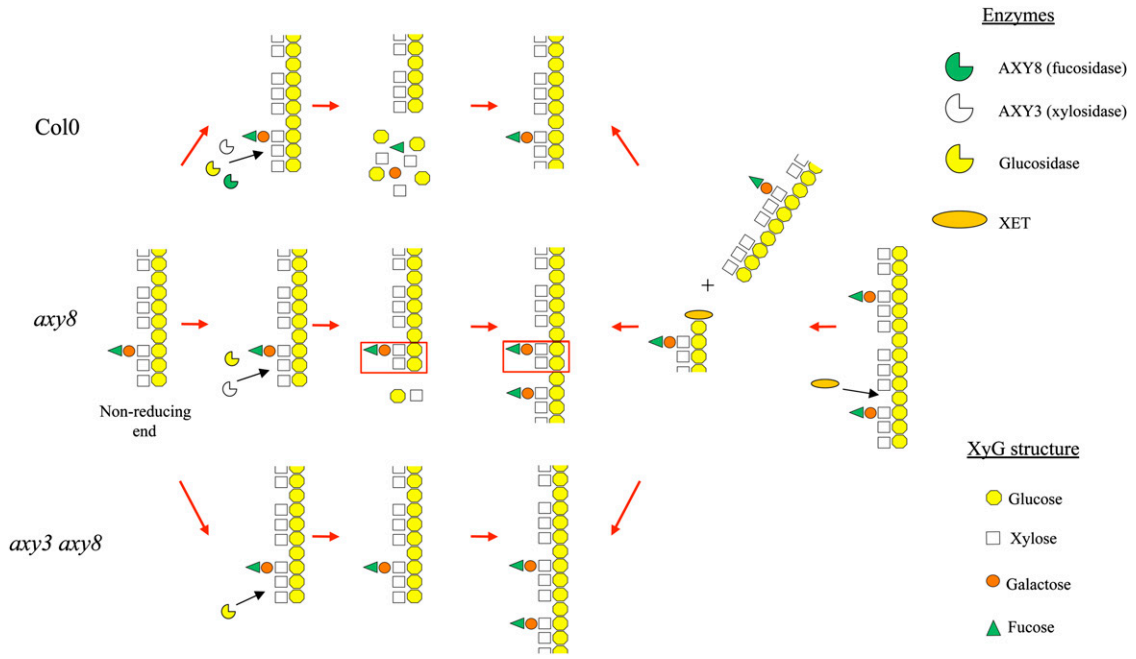

Figure 7. Metabolism of XyG in the Apoplast.

XyG is secreted into the apoplast consisting of a random pattern of only XXXG and XXFG (arrows pointing right). Apoplastic glycoside hydrolases can metabolize XyG from the nonreducing end. An active fucosidase is missing in the *axy8* mutant; *axy8 axy3* lacks both active fucosidase and xylosidase. In the wild type, XyG can be completely hydrolyzed to monosaccharides starting from the nonreducing end. In *axy8*, XyG can only be hydrolyzed incompletely; the lack of a fucosidase activity prevents the hydrolysis of side chains with a terminal fucosyl residue. Partially digested unusual XyG fragments can be detected (red rectangle). In the *axy3 axy8* double mutant, no XyG digestion occurs as terminal Xyl blocks XyG digestion.
Secreted XyG can be acted upon by an XET as described by Rose et al. (2002) (arrows pointing left). XET hydrolyzes the XyG polymer, forming a polymer-XET intermediate. The polysaccharide is then transferred to acceptor substrates such as XyG chains trimmed (or not) by glycosylhydrolases. The unusual XyG fragments can thus be incorporated into the polymer (red rectangle).

XyG has also been observed in the xylosidase mutant *axy3* (Günl and Pauly, 2011). Hence, apoplastic glycosylhydrolases are responsible for reducing the enzyme-accessible domains of XyG, likely to lock the polymer and make it more inert to metabolic events.

The Role of XyG in Plant Growth and Development

XyG has been proposed to be a major player in extension growth (Cosgrove, 1999). Evidence for this role is presented by the amount of XyG present in elongating tissues (Carpita and Gibeaut, 1993), structural alterations of XyG during cell elongation (Pauly et al., 2001), induction of the expression of genes involved in XyG metabolism during cell elongation and induction by auxin, a growth hormone (Sánchez et al., 2003), activities of XyG-acting enzymes in the elongation zone in vitro (Hensel et al., 1991) and in planta (Vissenberg et al., 2000), and modulation of cell elongation by XyG-derived oligosaccharides (Darvill et al., 1992; Takeda et al., 2002).

However, plant mutants with altered XyG structures have shown a surprising lack of a growth-related plant phenotype. In *mur1*, a mutant with a 98% reduction of XyG fucosylation in aerial plant parts, a mechanical weakness of the stem tissue, and plant dwarfism was observed (Reiter et al., 1993; Zablackis et al., 1996). However, this phenotype was later attributed to an alteration in the pectic polysaccharide rhamnogalacturonan II rather than XyG (O'Neill et al., 2001). Lack of XyG fucosyl substituents in *mur2* and an additional galactosyl residue in *mur3* did not cause the plants to display growth or morphological phenotypes (Madson et al., 2003; Perrin et al., 2003). However, on a cellular level, a defect in the organization of the endomembrane/actin system was demonstrated in *mur3* (Tamura et al., 2005), and on a macroscopic level, the mutant was found to resist infection in some tissues (Tedman-Jones et al., 2008). A XyG:xylosyltranferase mutant (*xxt5*) showed a root hair phenotype and alterations in primary root morphology (Zabotina et al., 2008). An insertional double mutant in the paralogs *xxt1*/*xxt2* also displayed a root hair phenotype (Cavalier et al., 2008), but otherwise no growth defects were observed despite the fact that this mutant lacks detectable levels of XyG. *axy8* follows this trend; despite significant changes in the XyG structure due to the presence of the unusual oligosaccharides and an increase in fucosylation, no growth or morphological phenotype was observed. *Arabidopsis* plants seem to be capable of tolerating significant structural or metabolic changes in both biosynthetic and apoplastic hydrolysis pathways. Whether plants compensate by altering

the structure, abundance, and/or macromolecular arrangement of other cell wall polysaccharides remains to be elucidated.

METHODS

Plant Material and Growth Conditions

The *axy3-1*, *axy8-1 axy8-4*, and *axy8-7* mutants were identified from an M2 EMS-mutagenized seed population (Berger and Altmann, 2000; Günl and Pauly, 2011). *axy8-1* was backcrossed three times to Col-0. T-DNA insertion mutants of *AXY8* were obtained from the GABI-Kat consortium (*axy8-5*, Gabi863G09; *axy8-6*, Gabi444B01). *axy3-1* etiolated seedlings were generated by placing surface-sterilized seeds on 0.5× Murashige and Skoog media plates (Murashige and Skoog, 1962) containing 1% (w/v) agar and 1% (w/v) Suc. After stratification for 2 to 3 d at 4°C in the dark, plant growth was induced briefly by light (6 h, 130 to 140 μmol m^{-2} s^{-1} light intensity) at 22°C. Plates were then darkened by wrapping three times with aluminum foil, and etiolated seedlings were grown for 4 to 7 d at 22°C.

Plants used for OLIMP analysis of leaf tissue and flower buds were grown under long-day conditions (16 h light/8 h dark) at 22°C with 170 to 190 μmol m^{-2} s^{-1} light intensity in environmentally controlled growth chambers.

Mapping of *axy8*

A mapping population for *axy8* was generated by crossing *axy8-1* (Col-0 background) to *Arabidopsis thaliana* cv Landsberg *erecta*. For the bulk segregant analysis using a microarray approach (Hazen et al., 2005), the XyG oligosaccharide composition of flowers of single plants from the F2 population was determined by OLIMP. Genomic DNA was prepared from the leaves of 50 plants with *axy8* XyG profiles and 50 with Col-0 XyG profiles, and 20 ng genomic DNA from each plant was pooled into two pools, one representing the wild-type phenotype and one representing *axy8*. Random labeling of genomic DNA was performed using the BioPrime DNA labeling system (Invitrogen). Concentrated random primers were added (60 μL) to 300 ng of genomic DNA together with water for a total volume of 132 μL. The mix was incubated for 10 min at 95°C and then cooled on ice. Ten times concentrated deoxynucleotide triphosphate mix with biotin dCTP (15 μL) and 3 μL of Klenow polymerase were added and incubated overnight at room temperature. The labeled products were purified by sodium ethanol precipitation using 15 μL of 3 M NaOAc and 400 μL of cold ethanol (absolute). The precipitated DNA was pelleted by centrifugation for 10 min at 20,000*g* and 4°C. The supernatant was discarded and the pellet was washed with 500 μL cold 75% aqueous ethanol. After another centrifugation step (10 min at 20,000*g* and 4°C), the pellet was air dried for 10 min at room temperature and resuspended in 100 μL water.The randomly labeled genomic DNA was hybridized to an Affymetrix ATH1 chip (Borevitz, 2006). For fine-mapping, the genetic background of individual F2 plants was determined by PCR-based marker analysis. Fine-mapping was performed on 960 F2 plants using the following markers: F17M5, T16L1, F28A23, F10M10, nga1139, and T4L20 (primer sequences in Supplemental Table 3 online). Mutations in the *AXY8* locus were identified and confirmed by sequencing.

Subcellular Localization

For the preparation of *AXY8* cDNA, RNA was extracted from 5-d-old Col-0 plants using Trizol reagent (Invitrogen). A cDNA library was then prepared using M-MLV reverse trancriptase (Invitrogen). The *AXY8* coding sequence was amplified from the cDNA library using Elongase enzyme (Invitrogen). The primers (see Supplemental Table 3 online) carried restriction sites for *Xba*I and *Sal*I. PCR products were cloned into pCR8/GW/TOPO. Following digestion of pCR8/GW/TOPO-AXY8 with *Xba*I and *Sal*I, the *AXY8* coding sequence was subcloned upstream of mGFP5 (Haseloff et al., 1997) into the binary vector pVKH18En6 (Batoko et al., 2000). The binary vector pVKH18En6-AXY8-GFP was transformed into *Agrobacterium tumefaciens* strain GVR101 and used for transient expression assays in 4-week-old *Nicotiana benthamiana* plants grown at 25°C. The bacterial optical density (OD_{600}) of the *Agrobacterium* used for plant transformation was 0.1. Three days after transformation, the plants were infiltrated with 10 μg /mL propidium iodide (MP Biomedical) or 25 μM FM 4-64 lipophilic dye (Life technologies), which stain the cell wall or the plasma membrane, respectively. To induce plasmolysis, leaf material was incubated for 10 min in a 1.5-mL tube with 1 M mannitol followed by wet mounting on a slide with 1 M mannitol. After these treatments, the abaxial plant epidermis was examined using a ×63 oil immersion objective on a Leica SD6000 microscope attached to a Yokogawa CSU-X1 spinning disc head with a 561-nm laser and controlled by Metamorph software. GFP was excited with an argon laser at 488 nm, and the signal was detected with a 525- to 550-nm band-pass filter. Propidium iodide and FM 4-64 were excited using an argon laser at 488 nm, and the signal was detected with a 620- to 660-nm band-pass filter. Confocal images were acquired using 400-ms exposure time, and bright-field images were acquired using 100-ms exposure time. Images were processed using ImageJ and all processing parameters kept constant across individual channels. In order to enhance visualization of colocalization, the merge pictures were individually adjusted using the color balance function of ImageJ.

Alternatively, a Zeiss 710 confocal laser scanning microscope was used to image the leaf material. Samples were excited with 488 nm, and emission was collected from 493 to 546 nm for the GFP channel (colored green) and 620 to 660 nm for the FM 4-64 channel (colored red). Image levels (max intensity, brightness, and contrast) were uniformly adjusted to improve visibility of GFP signal, and images were merged using ImageJ.

Overexpression of AXY8

The genomic region encompassing the *AXY8* gene was amplified by PCR using the BAC F10M10 as template using the primers shown in Supplemental Table 3 online. The PCR product was cloned into a TOPO-XL vector (Invitrogen) and transformed into *Escherichia coli* and the genomic sequence confirmed by sequencing. The gene was then excised from the TOPO-XL vector using the restriction sites *Kpn*I and *Sac*I introduced with the primers and cloned into pBINAR containing a 35S promoter (Höfgen and Willmitzer, 1990). The construct was then amplified in *E. coli* and transformed into *Agrobacterium* before transformation of *Arabidopsis* (Col-0; Weigel and Glazebrook, 2006).

Tissue Expression by GUS

For tissue expression studies using GUS, a 1.6-kb intergenic region upstream of *AXY8* was amplified from genomic DNA, introducing restriction sites for *Spe*I and *Bam*HI (see Supplemental Table 3 online). The PCR fragment was ligated into the pORE-R1 binary vector (Coutu et al., 2007) using the introduced restriction sites. The *AXY8* promoter:GUS construct was transformed into *Arabidopsis*, and transformants were selected by growing the T1 seeds on MS agar plates containing kanamycin (50 μg mL^{-1}). Resistant plants were transferred to soil, and T2 seeds were collected for GUS expression studies. Whole seedlings and roots were examined using the β-Glucuronidase Reporter Gene Staining Kit (GUSS-1KT; Sigma-Aldrich) according to the manufacturer's instructions.

The procedure for GUS staining of etiolated seedlings was adapted from Kim et al. (2006). Briefly, etiolated seedlings were grown for 5 d. Prefixation of the seedlings was performed for 20 min at room

temperature in 10 mM MES, pH 5.6, with 300 mM mannitol and 0.3% (v/v) formaldehyde. Samples were rinsed three times with distilled water and a staining solution was added (50 mM sodium phosphate buffer, pH 7.0, 0.2% [v/v] Triton X-100, 2 mM potassium ferrocyanide, and 2 mM potassium ferricyanide with 1.3 mM X-Gluc). Staining was performed at 37°C under slight agitation overnight. The staining solution was removed and the samples were fixed for 2 h with 2% (v/v) glutaraldehyde in 50 mM PIPES, pH 7.2, at 4°C. The samples were rinsed three times with 50 mM PIPES, pH 7.2. Seedlings were placed in 70% (v/v) ethanol, and staining was documented using a dissecting microscope.

Seedlings intended for sectioning were embedded in 1% (w/v) agarose (50 mM sodium phosphate buffer, pH 7.0) prior to prefixation and staining. Prefixation, staining, and postfixation were performed as described above. After postfixation and washing in 50 mM PIPES, pH 7.2, the samples were dehydrated in a graded series of ethanol-water (30, 40, 50, 60, 70, 80, and 95% [v/v]) with 15-min incubation at each step. This was followed by three incubations with anhydrous ethanol (15 min each). The ethanol was replaced with medium-grade LR White with LR White catalyst (Sigma-Aldrich), and the samples were placed under vacuum for 6 h at room temperature. The LR White was replaced with fresh LR White, and the samples were incubated overnight at room temperature. Single specimens were transferred to 1.5-mL microcentrifuge tubes, and LR White with catalyst and accelerator was added, covering the specimen. Sections of 5 μm were produced using a Leica RM2265 rotary microtome and stained with Safranin-O as described by Kim et al. (2006).

Transcript Analysis by RT-PCR

For *AXY8* expression analysis, RNA was extracted from 5-d-old etiolated seedlings using the RNeasy kit (Qiagen) following the instructions of the manufacturer. Total RNA was treated with DNase I (Roche) and transcribed into cDNA using Superscript II (Invitrogen) according to the guidelines of the manufacturers. For PCR reactions, JumpStart REDTaq ReadyMix PCR reagent (Sigma-Aldrich) was used in a total volume of 20 μL containing 0.5 μM forward and reverse primer and 1 μL cDNA template. Primer sequences can be found in the Supplemental Table 3 online. PCR reactions started with an initial heating step (5 min, 94°C), followed by 28 cycles consisting of denaturation (30 s, 94°C), annealing (30 s, 60°C), and extension (40 s, 72°C). The PCR concluded with a final incubation at 72°C for 10 min. PCR products were separated on a 4% agarose gel.

Fucosidase Activity Assay

Protein extraction was essentially performed as previously described (Sampedro et al., 2010). After grinding of ~1.2 g etiolated seedlings (4 d old) in liquid nitrogen, proteins were extracted with 9 mL of 50 mM sodium acetate buffer, pH 4.5, containing 1 M sodium chloride and 1× Halt Protease Inhibitor Cocktail (Thermo Scientific) for 2 h. The insoluble cell debris was removed by centrifugation, and the supernatant was concentrated in Amicon Ultra centrifugal filter units (Millipore) with a 10-kD molecular weight cutoff and washed twice with 10 mL 20 mM sodium acetate buffer, pH 5.0. The second wash contained 1× Halt Protease Inhibitor Cocktail. The extraction was performed at 4°C. The protein concentration was determined using the Bradford assay (Bio-Rad).

For α-1,2 fucosidase activity assays, 50 μL of 205 μM 2-fucosyllactose (Carbosynth) in 50 mM ammonium formate, pH 4.5, was digested overnight with 2 to 5 μg protein equivalents at 22°C. To avoid substrate depletion, activity assay for the *35S:AXY8* line was performed for 4 h. Released lactose was quantified using a HPAEC system (Dionex) equipped with a CarboPac PA200 coupled to a pulsed amperometric detector. Sugars were separated in a gradient for 9 min from 0 to 80 mM sodium acetate in 100 mM sodium hydroxide and a flow rate of 400 μL min^{-1}. The column was flushed with 300 mM sodium acetate in 100 mM sodium hydroxide for 4 min and then reequilibrated in 100 mM sodium hydroxide for 3 min after separation.

Preparation of Microsomes

Microsome extraction was adapted from Munoz et al. (1996) and Günl et al. (2011) with minor modifications. The complete procedure was performed at 4°C, and all solutions were prechilled. Briefly, ~10 to 20 g etiolated seedlings (4 d old) were finely chopped with a razor blade and homogenized with pestle and mortar in 8 mL 16% (w/v) Suc phosphate buffer (100 mM potassium phosphate buffer and 10 mM magnesium chloride, pH 6.65). After filtration through a nylon mesh, the extract was centrifuged for 10 min at 2000*g* and the supernatant was carefully transferred on top of a layer of 8 mL 38% (w/v) Suc phosphate buffer in 38.5-mL ultracentrifuge tubes (Beckman). After ultracentrifugation for 100 min at 100,000*g*, the microsomal layer above the 38% (w/v) Suc phosphate buffer was recovered with a Pasteur pipette and microsomes were diluted 1:2 with water. To pellet microsomes, samples were centrifuged for 60 min at 100,000*g*. After centrifugation, pellets were washed twice with 1 mL STM buffer (0.25 M Suc, 10 mM Tris-hydrochloride, and 1 mM magnesium chloride, pH 8.0). The pellet was eluted in 1 mL of STM buffer, and the protein concentration was determined by the Bradford assay (Bio-Rad).

Extraction of Alcohol-Insoluble Residue

Alcohol-insoluble residue (AIR) of whole-plant material was produced from as little as single etiolated seedlings up to as much as 80 mg of freeze-dried plant material. Plant material was snap frozen in liquid nitrogen and ground in a ball mill (Retsch) to a fine powder. After adding 1 mL of 70% (v/v) aqueous ethanol, samples were vortexed thoroughly and centrifuged (20,817 rcf, 10 min). After removal of the supernatant, samples were extracted with 1 mL 1:1 (v:v) chloroform: methanol. The supernatant was discarded and samples were dried. Extraction with each solvent was repeated until samples gave clear supernatants.

AIR from microsomal preparations was produced from a sample containing 100 μg protein equivalent. Microsome samples were dried by vacuum centrifugation and extracted once with 1 mL 1:1 (v:v) chloroform:methanol. After centrifugation (20,817 rcf, 10 min), 1 mL 80% (v/v) aqueous ethanol was added and samples were vortexed thoroughly and centrifuged for 10 min at 20,817 rcf. The supernatants were discarded, and samples were dried in a vacuum centrifuge.

OLIMP of XyG

OLIMP was performed as previously described (Günl et al., 2010). AIR derived from etiolated hypocotyls was digested overnight at 37°C with 0.2 units (1 unit releases 1 μmol XyG oligosaccharides per min) XEG in 50 μL of 50 mM ammonium formate, pH 4.5. EG digest was performed under the same conditions with 0.2 units (1 unit increases XyG reducing ends by 1 μmol per min) enzyme in 100 μL 50 mM ammonium formate. A portion of the supernatant (10 to 20 μL) containing the XyG oligosaccharides was desalted with ~10 conditioned BioRex MSZ 501 cation exchange beads (Bio-Rad). The desalted supernatant (2 μL) was spotted on top of 2 μL dried matrix (2,5-dihydroxybenzoic acid and 10 mg mL^{-1} in water) on a MALDI-TOF target plate. The drops were incubated for 5 min at room temperature and then dried quickly under vacuum. MALDI-TOF MS for OLIMP was performed on an AXIMA Performance (Shimadzu) instrument with an accelerating voltage of 20,000 V set to positive reflectron or linear mode.

OLIMP on leaf tissue was performed on ~100 μg AIR from 6-week-old plants. OLIMP analysis on flowers was performed on AIR obtained from four to five unopened flower buds from 6- to 9-week-old plants. AIR from microsomal fractions was digested at 37°C with 1 unit of XEG in 50 μL of 50 mM ammonium formate, pH 4.5.

Partial Purification and Analysis of Unusual XyG Oligosaccharides

For the purification/enrichment of the small (*m/z* <1700) unusual XyGOs from the *axy8* mutant, 80 to 120 mg AIR from etiolated seedlings was digested overnight at 37°C with 18 units of XEG in 50 mM ammonium formate, pH 4.5. The supernatant containing the solubilized XyG oligosaccharides was separated by centrifugation. The pellet was further extracted for 2 d at 4°C with 4 M potassium hydroxide. The supernatant of that treatment was neutralized with hydrochloric acid and desalted by dialysis of water under constant stirring using Slide-A-Lyzer dialysis cassettes (3500 molecular weight cutoff; Pierce) at 4°C. The resulting XyG polymer was digested overnight at 37°C with 18 units of XEG in 50 mM ammonium formate, pH 4.5. Both *axy8* XyG oligosaccharide extracts were combined and subjected to size exclusion chromatography on a FPLC (Bio-Rad) equipped with a Superdex Peptide column (10 mm ID × 300 mm; Amersham Pharmacia Biotech), using an isocratic flow (0.5 mL min^{-1}) of 50 mM ammonium formate, pH 5.0, and detection by refractive index (RI-71; Gynkotek). Collected fractions were monitored for XyG oligosaccharide content by MALDI-TOF MS. XyG oligosaccharides in some fractions were further fractionated using the FPLC system equipped with a reversed phase column (octadecyl [C-18], monomeric, 4.6 mm ID × 250 mm; Grace Vydac) using an elution gradient from 6 to 12% aqueous methanol within 60 min. Fractions were collected and monitored for XyG oligosaccharide content by MALDI-TOF MS. Ions corresponding to the mass of the unusual ions were present in two fractions, S1 and S2. The XyG oligosaccharide mixtures in these fractions were analyzed by ^{1}H-NMR as described (Jia et al., 2005). NMR spectra were recorded at 298K using a Varian Inova-600 MHz NMR spectrometer.

For the analysis of the unusual larger XyG oligosaccharides (>1700 D) occurring in *axy8*, AIR of etiolated seedlings was digested overnight at 37°C with 1 unit of XEG in 500 μL 50 mM ammonium formate, pH 4.5. The resulting XyG oligosaccharides were subjected to HPAEC (Dionex) with a CarboPac PA200 column connected to a pulsed amperometric detector. XyG oligosaccharides were eluted in 100 mM sodium hydroxide with a sodium acetate gradient of 0 to 80 mM within 20 min. Eluant between 18 and 22.5 min was collected and neutralized with acetic acid. The XyG oligosaccharides present in this fraction were desalted by solid-phase extraction on a tC18 96-well plate (Waters) as described by Hilz et al. (2007). The tC18 plate was preequilibrated with 400 μL water. After application of the XyG oligosaccharide solution, the plate was washed three times with water and the XyG oligosaccharides eluted in methanol (400 μL). XyG oligosaccharides were dried by vacuum centrifugation. The fraction with the enriched, large, unusual XyG oligosaccharides was reduced to its corresponding alditols for 1 h with 200 μL sodium borodeuteride (10 mg mL^{-1}) in 1 M ammonium hydroxide. After reduction, the samples were neutralized with acetic acid and residual borates were evaporated under a stream of nitrogen as methylesters. The presence of the large unusual oligosaccharides was confirmed by MALDI-TOF MS. Reduced XyG oligosaccharides were digested overnight at 37°C with 0.2 units of endo-1,4-β-glucanase from *Trichoderma longibrachiatum* (Megazyme) in 20 μL of 50 mM ammonium formate, pH 4.5.

For the determination of the XyG oligosaccharide order within the polymer, XyG was extracted from AIR prepared from 4-d etiolated seedlings of the *axy3-1 axy8-1* double mutant using 500 μL 4 M potassium hydroxide per 2 mg of AIR. After neutralization of the resulting supernatant with concentrated hydrochloric acid, XyG was precipitated by adding ethanol to a total of 70% (v/v) and stored overnight at 4°C. The precipitate was spun down for 10 min at 5920 rcf, and the pellet was washed three times with 10 mL 70% (v/v) aqueous ethanol. The XyG-containing pellet was dried and digested for various time points with 0.05 units of XEG at 37°C in 500 μL 50 mM ammonium formate, pH 4.5. A complete XyG digestion was performed using the same conditions but with 1 unit of XEG overnight.

XyG Oligosaccharide Composition by HPAEC-PAD

Absolute quantification of XyG oligosaccharides was performed by HPAEC-PAD as described by Günl and Pauly (2011). For the analysis of XEG-accessible XyG, 2 mg AIR of 4-d etiolated seedlings was digested overnight at 37°C with 1 unit of XEG in 500 μL 50 mM ammonium formate, pH 4.5. The supernatant was separated from the wall pellet by centrifugation and transferred to a new test tube. The remaining pellet containing XEG-inaccessible XyG was washed twice with 1 mL of water prior to alkaline extraction.

For the analysis of alkaline-extractable XyG, the XEG-treated pellet or 2 mg of AIR from 4-d-old etiolated seedlings was incubated with 500 μL 4 M potassium hydroxide. The samples were neutralized with hydrochloric acid after 4 h of incubation under vigorous shaking. The supernatants were collected after centrifugation and transferred to a new tube. The solubilized XyG was precipitated in 10 mL aqueous ethanol (70% [v/v] final concentration) overnight at 4°C. The XyG-containing pellet was washed three times with 10 mL 70% (v/v) aqueous ethanol and dried by vacuum centrifugation. The dried XyG polymer was digested at 37°C with 1 unit of XEG in 500 μL 50 mM ammonium formate, pH 4.5. The XyG oligosaccharide composition was determined by a HPAEC-PAD system (Dionex) using a CarboPac PA200 column. XyG oligosaccharides were separated in 100 mM sodium hydroxide in a gradient from 0 to 80 mM sodium acetate within 15 min at a flow rate of 400 μL min^{-1}. A standard curve based on XXXG (Megazyme) was used for quantification of the various XyG oligosaccharides. For the assignment of peaks, fractions (40 μL) were collected between 9 and 18.6 min for MALDI-TOF MS analysis. For desalting, 10 to 15 beads of conditioned Mixed bed resin TMD-8 (Sigma-Aldrich) were added to 20 to 30 μL of each fraction. XyGO compositions of fractions were determined by MALDI-TOF as described above. Furthermore, the retention times of eluted XyG oligosaccharides were compared with those of XyG oligosaccharide standards obtained by XEG digestion of *Arabidopsis* leaf AIR.

Cell Wall Monosaccharide Composition

Monosaccharide compositional analysis was performed on 2 mg of AIR from 4-d etiolated seedlings. Noncellulosic polysaccharides were hydrolyzed by 2 M trifluoroacetic acid, and the resulting monosaccharides were derivatized to alditol acetates and quantified by gas chromatography as described (Foster et al., 2010).

Accession Numbers

Sequence data from this article can be found in the Arabidopsis Genome Initiative or GenBank/EMBL databases under the following accession numbers: AXY8/Fuc95A, α-fucosidase, At4g34260; FXG1- XyG, fucosidase, At1g67830.

Supplemental Data

The following materials are available in the online version of this article.

Supplemental Figure 1. Isotopic Resolution of XXXG and XFG Oligosaccharides.

Supplemental Figure 2. Microarray and Marker-Assisted Identification of the *axy8* Mutation.

Supplemental Figure 3. Tissue Expression of *AXY8*.

Supplemental Figure 4. XyG Oligosaccharide OLIMP Profiles in Two Different Tissues of *axy8* and the Wild Type (Col-0).

Supplemental Figure 5. Transient Expression of *AXY8-GFP* in *Nicotiana benthamiana*.

Supplemental Figure 6. HPAEC-PAD Quantification of XyG Oligosaccharides.

Supplemental Table 1. XyG Oligosaccharide Composition of Wall Preparations from Etiolated Seedlings.

Supplemental Table 2. Monosaccharide Composition of Wall Preparations from Etiolated Seedlings (n = 3 to 4).

Supplemental Table 3. Oligonucleotide Sequences.

ACKNOWLEDGMENTS

We thank Kirk Schnorr (Novozymes, Bagsvaerd, Denmark) for the generous gift of XEG as well as Kerstin Zander, Peter Immerzeel, and Stefan Kühnel (all of the Max-Planck Institute for Molecular Plant Physiology) for excellent technical support. We also thank Greg Fedewa (Michigan State University) for technical assistance with the RT-PCR experiments. The genotyping of *axy8* was kindly performed by David Baker (John Innes Center Genome Lab, Norwich, UK). This work was supported by the Chemical Sciences, Geosciences, and Biosciences Division, Office of Basic Energy Sciences, Office of Science, U.S. Department of Energy (Award DE-FG02-91ER20021) and National Institutes of Health National Research Service Award Trainee appointment on Grant GM007127 to A.S.

AUTHOR CONTRIBUTIONS

M.G. wrote the article, designed and performed research, and analyzed the data (*axy* mutant spectra, *axy8* XyG characterization, *axy8 axy3* double mutant, and AXY8 overexpression line). L.N., F.K., A.d.S., A.S., M. Pena, and W.S.Y. designed and performed research and analyzed the data (L.N., fine-mapping of *axy8*, identification of the *axy8* mutation, and further characterization of *axy8* XyG oligosaccharides; F.K., *axy8* segregation analysis, microarray mapping of *axy8*, and GUS; A.D. and A.S., GFP localization studies; A.S., *Arabidopsis* XyG HPAEC standards; M. Pena and W.S.Y., NMR of unusual XyG oligosaccharides). M. Pauly wrote the article, designed research, performed experiments (mapping of *axy8*), and analyzed the data.

Received July 12, 2011; revised October 10, 2011; accepted October 25, 2011; published November 11, 2011.

REFERENCES

Anderson, C.T., Carroll, A., Akhmetova, L., and Somerville, C. (2010). Real-time imaging of cellulose reorientation during cell wall expansion in Arabidopsis roots. Plant Physiol. **152:** 787–796.

Batoko, H., Zheng, H.-Q., Hawes, C., and Moore, I. (2000). A rab1 GTPase is required for transport between the endoplasmic reticulum and golgi apparatus and for normal golgi movement in plants. Plant Cell **12:** 2201–2218.

Bauer, W.D., Talmadge, K.W., Keegstra, K., and Albersheim, P. (1973). The structure of plant cell walls: II. Hemicellulose of walls of suspension-cultured Sycamore cells. Plant Physiol. **51:** 174–187.

Berger, D., and Altmann, T. (2000). A subtilisin-like serine protease involved in the regulation of stomatal density and distribution in *Arabidopsis thaliana*. Genes Dev. **14:** 1119–1131.

Bonin, C.P., Potter, I., Vanzin, G.F., and Reiter, W.D. (1997). The *MUR1* gene of *Arabidopsis thaliana* encodes an isoform of GDP-D-mannose-4,6-dehydratase, catalyzing the first step in the *de novo* synthesis of GDP-L-fucose. Proc. Natl. Acad. Sci. USA **94:** 2085–2090.

Borevitz, J. (2006). Genotyping and mapping with high-density oligonucleotide arrays. Methods Mol. Biol. **323:** 137–145.

Burton, R.A., Gidley, M.J., and Fincher, G.B. (2010). Heterogeneity in the chemistry, structure and function of plant cell walls. Nat. Chem. Biol. **6:** 724–732.

Carpita, N.C., and Gibeaut, D.M. (1993). Structural models of primary cell walls in flowering plants: Consistency of molecular structure with the physical properties of the walls during growth. Plant J. **3:** 1–30.

Cavalier, D.M., Lerouxel, O., Neumetzler, L., Yamauchi, K., Reinecke, A., Freshour, G., Zabotina, O.A., Hahn, M.G., Burgert, I., Pauly, M., Raikhel, N.V., and Keegstra, K. (2008). Disrupting two *Arabidopsis thaliana* xylosyltransferase genes results in plants deficient in xyloglucan, a major primary cell wall component. Plant Cell **20:** 1519–1537.

Cosgrove, D.J. (1999). Enzymes and other agents that enhance cell wall extensibility. Annu. Rev. Plant Physiol. Plant Mol. Biol. **50:** 391–417.

Cosgrove, D.J. (2005). Growth of the plant cell wall. Nat. Rev. Mol. Cell Biol. **6:** 850–861.

Coutu, C., Brandle, J., Brown, D., Brown, K., Miki, B., Simmonds, J., and Hegedus, D.D. (2007). pORE: A modular binary vector series suited for both monocot and dicot plant transformation. Transgenic Res. **16:** 771–781.

Darvill, A., et al. (1992). Oligosaccharins—Oligosaccharides that regulate growth, development and defence responses in plants. Glycobiology **2:** 181–198.

de la Torre, F., Sampedro, J., Zarra, I., and Revilla, G. (2002). *AtFXG1*, an Arabidopsis gene encoding α-L-fucosidase active against fucosylated xyloglucan oligosaccharides. Plant Physiol. **128:** 247–255.

Fankhauser, N., and Mäser, P. (2005). Identification of GPI anchor attachment signals by a Kohonen self-organizing map. Bioinformatics **21:** 1846–1852.

Fincher, G.B. (2009). Revolutionary times in our understanding of cell wall biosynthesis and remodeling in the grasses. Plant Physiol. **149:** 27–37.

Foster, C.E., Martin, T.M., and Pauly, M. (March 12, 2010). Comprehensive compositional analysis of plant cell walls (lignocellulosic biomass) part II: carbohydrates. J. Vis. Exp. http://dx.doi.org/10.3791/1837.

Franková, L., and Fry, S.C. (2011). Phylogenetic variation in glycosidases and glycanases acting on plant cell wall polysaccharides, and the detection of transglycosidase and trans-β-xylanase activities. Plant J. **67:** 662–681.

Fry, S.C. (1989). The structure and functions of xyloglucan. J. Exp. Bot. **40:** 1–11.

Fry, S.C., Smith, R.C., Renwick, K.F., Martin, D.J., Hodge, S.K., and Matthews, K.J. (1992). Xyloglucan endotransglycosylase, a new wall-loosening enzyme activity from plants. Biochem. J. **282:** 821–828.

Fry, S.C., et al. (1993). An unambiguous nomenclature for xyloglucan-derived oligosaccharides. Physiol. Plant. **89:** 1–3.

Gibeaut, D.M., Pauly, M., Bacic, A., and Fincher, G.B. (2005). Changes in cell wall polysaccharides in developing barley (*Hordeum vulgare*) coleoptiles. Planta **221:** 729–738.

Gille, S., Souza, A., Xiong, G., Benz, M., Schultink, A., Ida-Reca, B., and Pauly, M. (2011). O-acetylation of *Arabidopsis* hemicellulose

xyloglucan requires AXY4 or AXY4L, proteins with a TBL and DUF231 domain. Plant Cell **23:** 4041–4053.

Guillén, R., York, W.S., Pauly, M., An, J., Impallomeni, G., Albersheim, P., and Darvill, A.G. (1995). Metabolism of xyloglucan generates xylose-deficient oligosaccharide subunits of this polysaccharide in etiolated peas. Carbohydr. Res. **277:** 291–311.

Günl, M., Gille, S., and Pauly, M. (2010). OLIgo mass profiling (OLIMP) of extracellular polysaccharides. J. Vis. Exp. (40): 10.3791/2046.

Günl, M., Kraemer, F., and Pauly, M. (2011). Oligosaccharide mass profiling (OLIMP) of cell wall polysaccharides by MALDI-TOF/MS. In The Plant Cell Wall: Methods and Protocols, Z. Popper, ed (New York City: Humana Press), pp. 43–54.

Günl, M., and Pauly, M. (2011). *AXY3* encodes a α-xylosidase that impacts the structure and accessibility of the hemicellulose xyloglucan in Arabidopsis plant cell walls. Planta **233:** 707–719.

Haseloff, J., Siemering, K.R., Prasher, D.C., and Hodge, S. (1997). Removal of a cryptic intron and subcellular localization of green fluorescent protein are required to mark transgenic Arabidopsis plants brightly. Proc. Natl. Acad. Sci. USA **94:** 2122–2127.

Hayashi, T. (1989). Xyloglucans in the primary cell wall. Annu. Rev. Plant Physiol. Plant Mol. Biol. **40:** 139–168.

Hazen, S.P., Borevitz, J.O., Harmon, F.G., Pruneda-Paz, J.L., Schultz, T.F., Yanovsky, M.J., Liljegren, S.J., Ecker, J.R., and Kay, S.A. (2005). Rapid array mapping of circadian clock and developmental mutations in Arabidopsis. Plant Physiol. **138:** 990–997.

Hensel, A., Brummell, D.A., Hanna, R., and Maclachlan, G. (1991). Auxin-dependent breakdown of xyloglucan in cotyledons of germinating nasturtium seeds. Planta **183:** 321–326.

Hilz, H., de Jong, L.E., Kabel, M.A., Verhoef, R., Schols, H.A., and Voragen, A.G.J. (2007). Bilberry xyloglucan—Novel building blocks containing β-xylose within a complex structure. Carbohydr. Res. **342:** 170–181.

Hoffman, M., Jia, Z., Peña, M.J., Cash, M., Harper, A., Blackburn II, A.R., Darvill, A., and York, W.S. (2005). Structural analysis of xyloglucans in the primary cell walls of plants in the subclass *Asteridae*. Carbohydr. Res. **340:** 1826–1840.

Höfgen, R., and Willmitzer, L. (1990). Biochemical and genetic analysis of different patatin isoforms expressed in various organs of potato (*Solanum tuberosum*). Plant Sci. **66:** 221–230.

Iglesias, N., Abelenda, J.A., Rodiño, M., Sampedro, J., Revilla, G., and Zarra, I. (2006). Apoplastic glycosidases active against xyloglucan oligosaccharides of *Arabidopsis thaliana*. Plant Cell Physiol. **47:** 55–63.

Jia, Z., Cash, M., Darvill, A.G., and York, W.S. (2005). NMR characterization of endogenously *O*-acetylated oligosaccharides isolated from tomato (*Lycopersicon esculentum*) xyloglucan. Carbohydr. Res. **340:** 1818–1825.

Kiefer, L.L., York, W.S., Darvill, A.G., and Albersheim, P. (1989). Xyloglucan isolated from suspension-cultured sycamore cell-walls is *O*-acetylated. Phytochemistry **28:** 2105–2107.

Kim, K.-W., Franceschi, V.R., Davin, L.B., and Lewis, N.G. (2006). β-Glucuronidase as reporter gene. In Methods in Molecular Biology, J. Salinas and J.J. Sanchez-Serrano, eds (Totowa, NJ: Humana Press), pp. 263–273.

Leboeuf, E., Immerzeel, P., Gibon, Y., Steup, M., and Pauly, M. (2008). High-throughput functional assessment of polysaccharide-active enzymes using matrix-assisted laser desorption/ionization-time-of-flight mass spectrometry as exemplified on plant cell wall polysaccharides. Anal. Biochem. **373:** 9–17.

Léonard, R., Pabst, M., Bondili, J.S., Chambat, G., Veit, C., Strasser, R., and Altmann, F. (2008). Identification of an Arabidopsis gene encoding a GH95 α1,2-fucosidase active on xyloglucan oligo- and polysaccharides. Phytochemistry **69:** 1983–1988.

Lerouxel, O., Cavalier, D.M., Liepman, A.H., and Keegstra, K. (2006). Biosynthesis of plant cell wall polysaccharides - A complex process. Curr. Opin. Plant Biol. **9:** 621–630.

Lerouxel, O., Choo, T.S., Séveno, M., Usadel, B., Faye, L., Lerouge, P., and Pauly, M. (2002). Rapid structural phenotyping of plant cell wall mutants by enzymatic oligosaccharide fingerprinting. Plant Physiol. **130:** 1754–1763.

Levy, S., Maclachlan, G., and Staehelin, L.A. (1997). Xyloglucan sidechains modulate binding to cellulose during *in vitro* binding assays as predicted by conformational dynamics simulations. Plant J. **11:** 373–386.

Lorences, E.P., and Fry, S.C. (1993). Xyloglucan oligosaccharides with at least two α-D-xylose residues act as acceptor substrates for xyloglucan endotransglycosylase and promote the depolymerisation of xyloglucan. Physiol. Plant. **88:** 105–112.

Madson, M., Dunand, C., Li, X., Verma, R., Vanzin, G.F., Caplan, J., Shoue, D.A., Carpita, N.C., and Reiter, W.-D. (2003). The *MUR3* gene of Arabidopsis encodes a xyloglucan galactosyltransferase that is evolutionarily related to animal exostosins. Plant Cell **15:** 1662–1670.

Moore, P.J., Swords, K.M., Lynch, M.A., and Staehelin, L.A. (1991). Spatial organization of the assembly pathways of glycoproteins and complex polysaccharides in the Golgi apparatus of plants. J. Cell Biol. **112:** 589–602.

Munoz, P., Norambuena, L., and Orellana, A. (1996). Evidence for a UDP-glucose transporter in Golgi apparatus-derived vesicles from pea and its possible role in polysaccharide biosynthesis. Plant Physiol. **112:** 1585–1594.

Murashige, T., and Skoog, F. (1962). A revised medium for rapid growth and bioassays with tobacco tissue cultures. Physiol. Plant. **15:** 473–497.

Neumetzler, L. (2010). Identification and Characterization of Arabidopsis Mutants Associated with Xyloglucan Metabolism. (Berlin: Rhombos Publishing).

Nishitani, K., and Tominaga, R. (1992). Endo-xyloglucan transferase, a novel class of glycosyltransferase that catalyzes transfer of a segment of xyloglucan molecule to another xyloglucan molecule. J. Biol. Chem. **267:** 21058–21064.

Obel, N., Erben, V., Schwarz, T., Kühnel, S., Fodor, A., and Pauly, M. (2009). Microanalysis of plant cell wall polysaccharides. Mol. Plant **2:** 922–932.

O'Neill, M.A., Eberhard, S., Albersheim, P., and Darvill, A.G. (2001). Requirement of borate cross-linking of cell wall rhamnogalacturonan II for Arabidopsis growth. Science **294:** 846–849.

Pauly, M., Albersheim, P., Darvill, A., and York, W.S. (1999a). Molecular domains of the cellulose/xyloglucan network in the cell walls of higher plants. Plant J. **20:** 629–639.

Pauly, M., Andersen, L.N., Kauppinen, S., Kofod, L.V., York, W.S., Albersheim, P., and Darvill, A. (1999b). A xyloglucan-specific *endo*-β-1,4-glucanase from *Aspergillus aculeatus*: expression cloning in yeast, purification and characterization of the recombinant enzyme. Glycobiology **9:** 93–100.

Pauly, M., Qin, Q., Greene, H., Albersheim, P., Darvill, A., and York, W.S. (2001). Changes in the structure of xyloglucan during cell elongation. Planta **212:** 842–850.

Perrin, R.M., DeRocher, A.E., Bar-Peled, M., Zeng, W., Norambuena, L., Orellana, A., Raikhel, N.V., and Keegstra, K. (1999). Xyloglucan fucosyltransferase, an enzyme involved in plant cell wall biosynthesis. Science **284:** 1976–1979.

Perrin, R.M., Jia, Z., Wagner, T.A., O'Neill, M.A., Sarria, R., York, W.S., Raikhel, N.V., and Keegstra, K. (2003). Analysis of xyloglucan fucosylation in Arabidopsis. Plant Physiol. **132:** 768–778.

Reiter, W.D., Chapple, C.C.S., and Somerville, C.R. (1993). Altered growth and cell walls in a fucose-deficient mutant of Arabidopsis. Science **261:** 1032–1035.

Reiter, W.D., Chapple, C.C.S., and Somerville, C.R. (1997). Mutants of

Arabidopsis thaliana with altered cell wall polysaccharide composition. Plant J. **12:** 335–345.

Rose, J.K.C., Braam, J., Fry, S.C., and Nishitani, K. (2002). The XTH family of enzymes involved in xyloglucan endotransglucosylation and endohydrolysis: Current perspectives and a new unifying nomenclature. Plant Cell Physiol. **43:** 1421–1435.

Sampedro, J., Pardo, B., Gianzo, C., Guitián, E., Revilla, G., and Zarra, I. (2010). Lack of α-xylosidase activity in Arabidopsis alters xyloglucan composition and results in growth defects. Plant Physiol. **154:** 1105–1115.

Sampedro, J., Sieiro, C., Revilla, G., González-Villa, T., and Zarra, I. (2001). Cloning and expression pattern of a gene encoding an α-xylosidase active against xyloglucan oligosaccharides from Arabidopsis. Plant Physiol. **126:** 910–920.

Sánchez, M., Gianzo, C., Sampedro, J., Revilla, G., and Zarra, I. (2003). Changes in α-xylosidase during intact and auxin-induced growth of pine hypocotyls. Plant Cell Physiol. **44:** 132–138.

Scheible, W.R., and Pauly, M. (2004). Glycosyltransferases and cell wall biosynthesis: Novel players and insights. Curr. Opin. Plant Biol. **7:** 285–295.

Scheller, H.V., and Ulvskov, P. (2010). Hemicelluloses. Annu. Rev. Plant Biol. **61:** 263–289.

Schwacke, R., Schneider, A., van der Graaff, E., Fischer, K., Catoni, E., Desimone, M., Frommer, W.B., Flügge, U.I., and Kunze, R. (2003). ARAMEMNON, a novel database for Arabidopsis integral membrane proteins. Plant Physiol. **131:** 16–26.

Smith, R.C., and Fry, S.C. (1991). Endotransglycosylation of xyloglucans in plant cell suspension cultures. Biochem. J. **279:** 529–535.

Spronk, B.A., Rademaker, G.J., Haverkamp, J., Thomas-Oates, J.E., Vincken, J.-P., Voragen, A.G.J., Kamerling, J.P., and Vliegenthart, J.F.G. (1997). Dimers of a GFG hexasaccharide occur in apple fruit xyloglucan. Carbohydr. Res. **305:** 233–242.

Takeda, T., Furuta, Y., Awano, T., Mizuno, K., Mitsuishi, Y., and Hayashi, T. (2002). Suppression and acceleration of cell elongation by integration of xyloglucans in pea stem segments. Proc. Natl. Acad. Sci. USA **99:** 9055–9060.

Tamura, K., Shimada, T., Kondo, M., Nishimura, M., and Hara-Nishimura, I. (2005). KATAMARI1/MURUS3 Is a novel golgi membrane protein that is required for endomembrane organization in *Arabidopsis*. Plant Cell **17:** 1764–1776.

Tedman-Jones, J.D., Lei, R., Jay, F., Fabro, G., Li, X.M., Reiter, W.D., Brearley, C., and Jones, J.D.G. (2008). Characterization of Arabidopsis *mur3* mutations that result in constitutive activation of defence in petioles, but not leaves. Plant J. **56:** 691–703.

Thompson, J.E., and Fry, S.C. (2001). Restructuring of wall-bound xyloglucan by transglycosylation in living plant cells. Plant J. **26:** 23–34.

Vanzin, G.F., Madson, M., Carpita, N.C., Raikhel, N.V., Keegstra, K., and Reiter, W.-D. (2002). The *mur2* mutant of *Arabidopsis thaliana* lacks fucosylated xyloglucan because of a lesion in fucosyltransferase AtFUT1. Proc. Natl. Acad. Sci. USA **99:** 3340–3345.

Vincken, J.P., York, W.S., Beldman, G., and Voragen, A.G.J. (1997). Two general branching patterns of xyloglucan, XXXG and XXGG. Plant Physiol. **114:** 9–13.

Vissenberg, K., Fry, S.C., Pauly, M., Höfte, H., and Verbelen, J.P. (2005). XTH acts at the microfibril-matrix interface during cell elongation. J. Exp. Bot. **56:** 673–683.

Vissenberg, K., Martinez-Vilchez, I.M., Verbelen, J.-P., Miller, J.G., and Fry, S.C. (2000). *In vivo* colocalization of xyloglucan endotransglycosylase activity and its donor substrate in the elongation zone of *Arabidopsis* roots. Plant Cell **12:** 1229–1237.

Weigel, D., and Glazebrook, J. (2006). In planta transformation of Arabidopsis. Cold Spring Harb. Protoc. http://dx.doi.org/10.1101/pdb.prot4668.

York, W.S., Darvill, A.G., and Albersheim, P. (1984). Inhibition of 2,4-dichlorophenoxyacetic acid-stimulated elongation of pea stem segments by a xyloglucan oligosaccharide. Plant Physiol. **75:** 295–297.

York, W.S., Kumar Kolli, V.S., Orlando, R., Albersheim, P., and Darvill, A.G. (1996). The structures of arabinoxyloglucans produced by solanaceous plants. Carbohydr. Res. **285:** 99–128.

Zablackis, E., York, W.S., Pauly, M., Hantus, S., Reiter, W.D., Chapple, C.C.S., Albersheim, P., and Darvill, A. (1996). Substitution of L-fucose by L-galactose in cell walls of Arabidopsis *mur1*. Science **272:** 1808–1810.

Zabotina, O.A., van de Ven, W.T., Freshour, G., Drakakaki, G., Cavalier, D., Mouille, G., Hahn, M.G., Keegstra, K., and Raikhel, N.V. (2008). Arabidopsis *XXT5* gene encodes a putative α-1,6-xylosyltransferase that is involved in xyloglucan biosynthesis. Plant J. **56:** 101–115.